

Accepted Manuscript

Design, synthesis and molecular modeling of new 4-phenylcoumarin derivatives as tubulin polymerization inhibitors targeting MCF-7 breast cancer cells

Rasha Z. Batran, Asmaa F. Kassem, Eman M. Abbas, Samia A. El Seginy, Marwa M. Mounier

PII: S0968-0896(18)30745-4
DOI: <https://doi.org/10.1016/j.bmc.2018.05.022>
Reference: BMC 14364

To appear in: *Bioorganic & Medicinal Chemistry*

Received Date: 17 April 2018
Revised Date: 13 May 2018
Accepted Date: 15 May 2018

Please cite this article as: Batran, R.Z., Kassem, A.F., Abbas, E.M., El Seginy, S.A., Mounier, M.M., Design, synthesis and molecular modeling of new 4-phenylcoumarin derivatives as tubulin polymerization inhibitors targeting MCF-7 breast cancer cells, *Bioorganic & Medicinal Chemistry* (2018), doi: <https://doi.org/10.1016/j.bmc.2018.05.022>

This is a PDF file of an unedited manuscript that has been accepted for publication. As a service to our customers we are providing this early version of the manuscript. The manuscript will undergo copyediting, typesetting, and review of the resulting proof before it is published in its final form. Please note that during the production process errors may be discovered which could affect the content, and all legal disclaimers that apply to the journal pertain.



Design, synthesis and molecular modeling of new 4-phenylcoumarin derivatives as tubulin polymerization inhibitors targeting MCF-7 breast cancer cells

**Rasha Z. Batran,^a Asmaa F. Kassem,^{b*} Eman M. Abbas,^b Samia A. El Seginy,^c
Marwa M. Mounier^d**

^a *Chemistry of Natural Compounds Department, Pharmaceutical and Drug Industries Research Division, National Research Centre, 33 El Bohouth St., Dokki, Giza, P.O. Box 12622, Egypt*

^b *Chemistry of Natural and Microbial Products Department, Pharmaceutical and Drug Industries Research Division, National Research Centre, 33 El Bohouth St., Dokki, Giza, P.O. Box 12622, Egypt*

^c *Green Chemistry Department, Chemical Industries Research Division, National Research Centre, 33 El Bohouth St., Dokki, Giza, p. o. box 12622, Egypt*

^d *Pharmacognosy Department, Drug Bioassay-Cell Culture Laboratory, Pharmaceutical and Drug Industries Research Division, National Research Centre, 33 El Bohouth St., Dokki, Giza, P.O. Box 12622, Egypt*

Corresponding author: asmaa.kassem@yahoo.com

Abstract

A new set of 4-phenylcoumarin derivatives was designed and synthesized aiming to introduce new tubulin polymerization inhibitors as anti-breast cancer candidates. All the target compounds were evaluated for their cytotoxic effects against MCF-7 cell line, where compounds **2f**, **3a**, **3b**, **3 f**, **7a** and **7b**, showed higher cytotoxic effect ($IC_{50}=4.3-21.2 \mu\text{g/mL}$) than the reference drug doxorubicin ($IC_{50}= 26.1 \mu\text{g/mL}$), additionally, compounds **1** and **6b** exhibited the same potency as doxorubicin ($IC_{50}= 25.2$ and $28.0 \mu\text{g/mL}$, respectively). The thiazolidinone derivatives **3a**, **3b** and **3 f** with potent and selective anticancer effects towards MCF-7 cells ($IC_{50} = 11.1, 16.7$ and $21.2 \mu\text{g/mL}$) were further assessed for tubulin polymerization inhibition effects which showed that the three compounds were potent tubulin polymerization suppressors with IC_{50} values of $9.37, 2.89$ and $6.13 \mu\text{M}$, respectively, compared to the reference drug colchicine ($IC_{50}= 6.93 \mu\text{M}$). The mechanistic effects on cell cycle progression and induction of apoptosis in MCF-7 cells were determined for compound **3a** due to its potent and selective cytotoxic effects

in addition to its promising tubulin polymerization inhibition potency. The results revealed that compound **3a** induced cell cycle cessation at G2/M phase and accumulation of cells in pre-G1 phase and prevented its mitotic cycle, in addition to its activation of caspase-7 mediating apoptosis of MCF-7 cells. Molecular modeling studies for compounds **3a**, **3b** and **3 f** were carried out on tubulin crystallography, the results indicated that the compounds showed binding mode similar to the co-crystallized ligand; colchicine. Moreover, pharmacophore constructed models and docking studies revealed that thiazolidinone, acetamide and coumarin moieties are crucial for the activity. Molecular dynamics (MD) studies were carried out for the three compounds over 100Ps. MD results of compound **3a** showed that it reached the stable state after 30Ps which was in agreement with the calculated potential and kinetic energy of compound **3a**.

Keywords: 4-phenylcoumarins; thiazole; MCF-7; tubulin polymerization; apoptosis; molecular modeling.

1. Introduction

The microtubule network is a fundamental element of the cytoskeleton of eukaryotic cells which is involved in various biological processes. Microtubules are assembled from heterodimers of α and β tubulin.¹ The cycle of microtubule assembly and disassembly is basically regulated by microtubule-associated proteins as MAP1A, MAP1A B, stathmin or tau.²⁻⁵ Colchicine, *vinca*-alkaloids and taxane are examples of therapeutic anticancer agents targeting the microtubule cytoskeleton.⁶⁻⁸

The discovery of colchicine binding to tubulin was a crucial step in the development of antimetabolic drugs.⁹ Among the different antimetabolic agents that inhibit tubulin polymerization *via* interaction with the colchicine binding site, combretastatin derivatives represent the most widely investigated class of antimetabolic agents since the discovery of combretastatin A-4 (CA-4), a natural antimetabolic and anti-angiogenic agent isolated from the bark of the African willow tree *Combretum cafferum* (**Fig.1A**).¹⁰⁻¹³

The development of new antimetabolic agents has led to new approaches of cancer chemotherapy and advanced knowledge of microtubule biochemistry and pharmacology. Recently, several studies have focused on the advanced clinical trial development of new candidates as combretastatin AVE 8062A, combretastatin A-4 phosphate (CA-4P) and combretastatin A1 diphosphate (OXi 4503) (**Fig.1B**).¹⁴⁻¹⁷

Structural modifications of CA-4 lead to the identification of new combretastatin-A4 thiazole/ thiazolidinone hybrids as tubulin targeting antimetabolic agents acting through the colchicine binding site of tubulin and causing disruption in microtubule assembly and dynamics. (**Fig.1C**).¹⁸⁻²¹

On the other hand, coumarins are a class of naturally occurring compounds with diverse pharmacological effects, especially in the field of anticancer therapy.²²⁻²⁸ 4-Arylcoumarins, known as neoflavones have been reported for their antimetabolic effects.²⁹⁻³¹ Due to structural similarity, 4-arylcoumarins share the colchicine binding domain with the natural antimetabolic agent combretastatin A-4.^{30,32} Moreover, the rigid conformation of 4-phenylcoumarin backbone avoids the biological inactivation resulting from the inherent conformational instability of combretastatin scaffold due to the cis-trans isomerization about the ethylene linker (**Fig. 1D**).^{33,34}

Hybridization of two or more scaffolds in one candidate molecule represents efficient hybrid pharmacophore approach for the development of new antitumor agents. Previous structure activity relationship studies of 4-arylcoumarin as tubulin inhibitors revealed that direct substitution on ring A, particularly with methoxy groups, has an essential effect on tubulin polymerization and antitumor effect.²⁹⁻³¹ However, no reports have considered the conjugation of the 4-phenylcoumarin scaffold and other bioactive heterocyclic moieties.

With this aspect we focused on the synthesis of a new series of 4-phenylcoumarin analogues hybridized with the heterocyclic thiazole and thiazolidinone moieties through acetamide or acetohydrazide linker. All target compounds were assessed for their cytotoxic effects against human breast cancer cell line MCF-7 and the potent antiproliferative candidates were further examined as tubulin polymerization suppressors. Furthermore, the mechanistic effects of the most active derivative were evaluated regarding cell cycle analysis, apoptosis and caspase-7 detection. Molecular modeling study was carried out for the promising compounds to explore the plausible binding modes in the tubulin active site and molecular dynamics simulation was also performed to evaluate their binding stability.

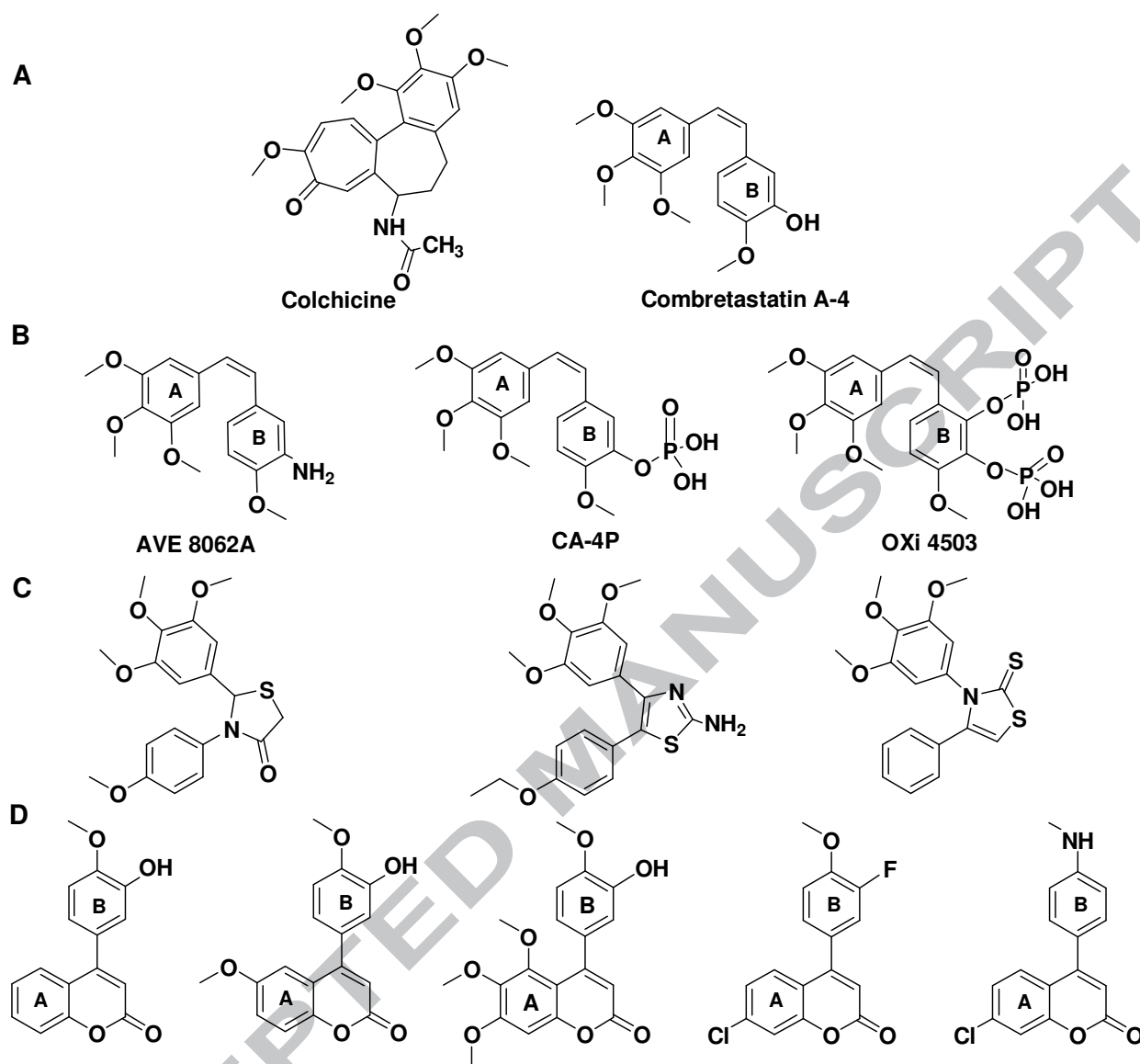


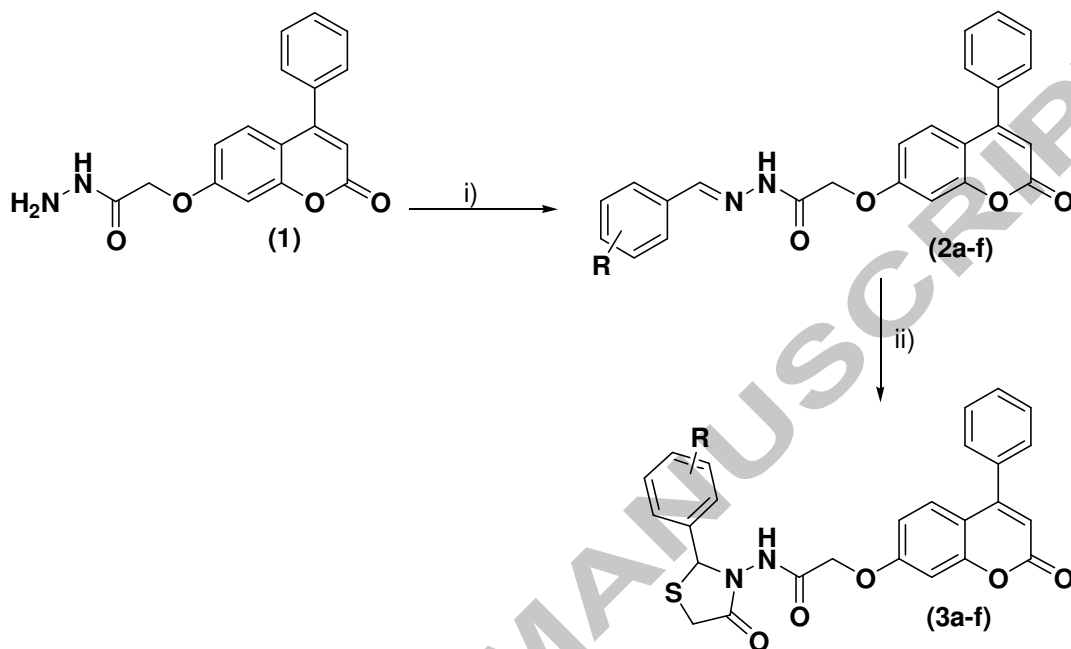
Fig.1. Tubulin polymerization inhibitors. **A)** Structures of known inhibitors, **B)** Structures of inhibitors in clinical trials, **C)** Combretastatin-A4 thiazole/ thiazolidinone hybrids, **D)** Structures of 4-aryl coumarin derivatives.

2. Results and Discussion

2.1. Chemistry

The preparation of 4-phenyl-7-oxycoumarin derivatives **1**, **2a-f**, **3a-f**, **4a,b**, **5a,b**, **6a,b**, **7a,b**, **8a,b**, **9a,b** and **10a,b** was outlined in Schemes 1-3. The Schiff's bases **2a-f** were synthesized through the reaction of hydrazide **1** with different aromatic aldehydes, namely; 4-fluorobenzaldehyde, 4-chlorobenzaldehyde, 4-bromobenzaldehyde, 4-anisaldehyde, 3,4-

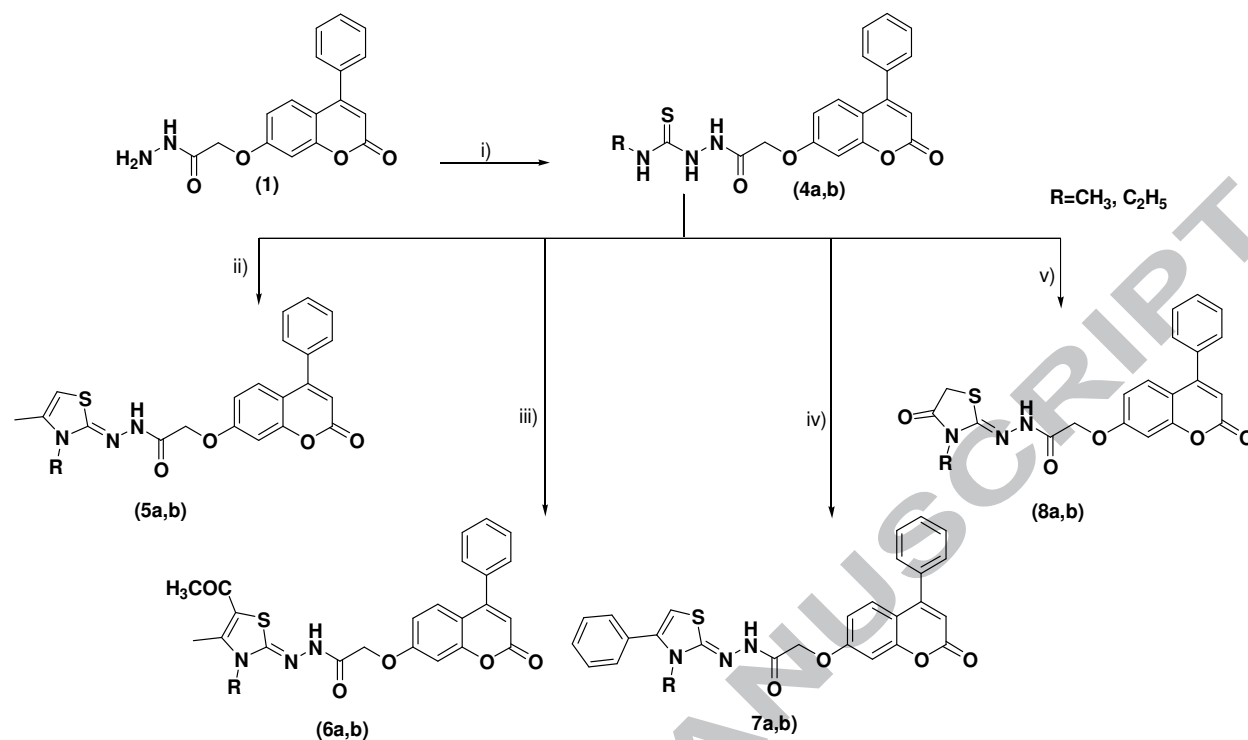
dimethoxybenzaldehyde and /or 3,4,5-trimethoxybenzaldehyde. Cyclocondensation of the synthesized Schiff's bases **2a-f** with thioglycolic acid in refluxing benzene afforded the corresponding thiazolidinone derivatives **3a-f** (Scheme 1).



R=4-F, 4-Cl,4-Br, 4-OCH₃, 3,4-(OCH₃)₂, 3,4,5-(OCH₃)₃

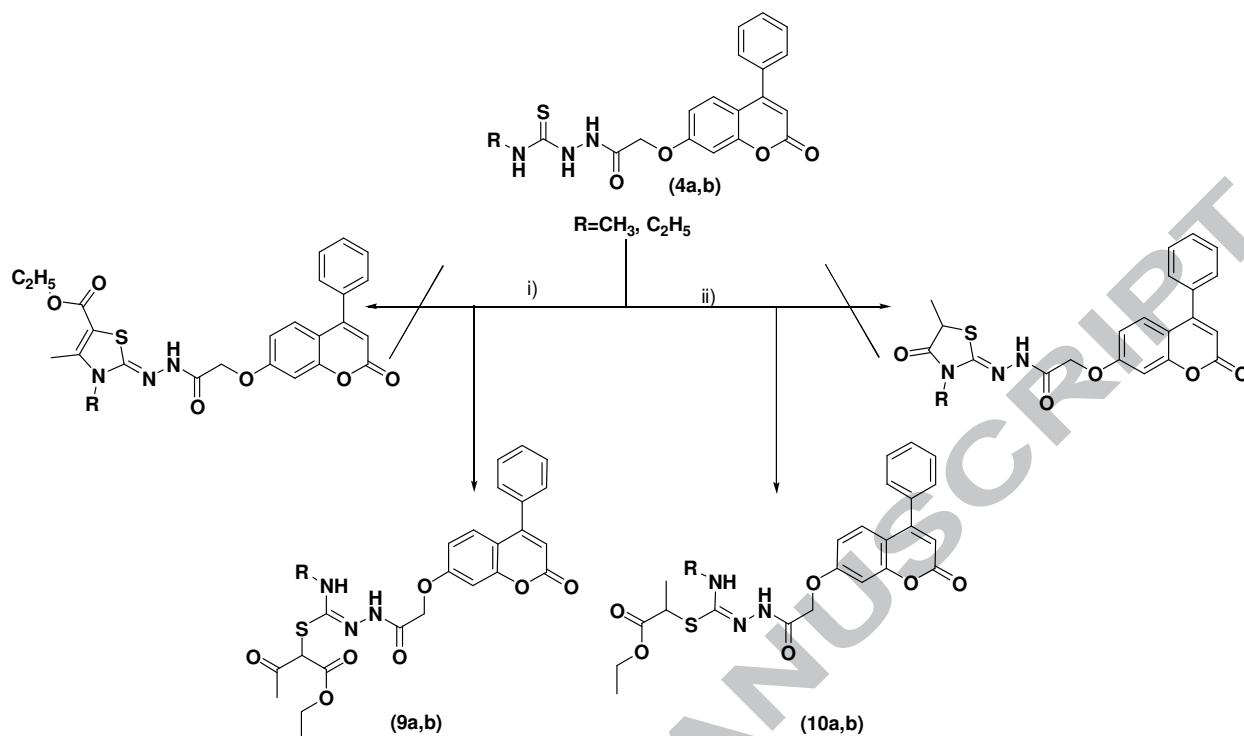
Scheme 1. i) ArCHO, EtOH, CH₃COOH, reflux, ii) HSCH₂COOH, benzene, reflux

Condensation reaction of the hydrazide **1** with methyl isothiocyanate and/or ethyl isothiocyanate yielded the thiosemicarbazide derivatives **4a,b**. Heterocyclization of the prepared thiosemicarbazide derivatives **4a,b** with the appropriate α -halocarbonyl compounds, namely; chloroacetone, 3-chloroacetylacetone and/ or phenacyl bromide, in refluxing ethanol and catalytic amount of anhydrous sodium acetate afforded the corresponding thiazoline derivatives **5a,b** -**7a,b**. Similarly, the thiazolidinones **8a,b** were synthesized *via* refluxing **4a,b** with ethyl bromoacetate in the presence of anhydrous sodium acetate. These reactions were assumed to proceed through S-alkylation reaction followed by dehydration or loss of an alcohol molecule (Scheme 2).



Scheme 2. i) RNCS, EtOH, reflux, ii) CH₃COCH₂Cl, CH₃COONa, EtOH, reflux, iii) CH₃COCH(Cl)COCH₃, CH₃COONa, EtOH, reflux, iv) PhCOCH₂Br, CH₃COONa, EtOH, reflux, v) CH₃CH₂OCOCH₂Br, CH₃COONa, EtOH, reflux.

On the other hand, the reaction of the key intermediates **4a,b** with ethyl-2-chloroacetoacetate and ethyl-2-bromopropionate in absolute ethanol in the presence of anhydrous sodium acetate proceeded via S-alkylation reaction without further dehydration or loss of alcohol molecule to afford the unexpected open chain derivatives **9a,b** and **10a,b**, respectively (**Scheme 3**). The structures of the newly synthesized target compounds were elucidated by IR, ¹H NMR, ¹³C NMR and EI-MS (Experimental section).



Scheme 3. i) $\text{CH}_3\text{COCH}(\text{Cl})\text{COOC}_2\text{H}_5$, CH_3COONa , EtOH, reflux, ii) $\text{BrCH}(\text{CH}_3)\text{COOC}_2\text{H}_5$, CH_3COONa , EtOH, reflux.

2.2. Biology

2.2.1. *In vitro* anticancer activity against breast cancer cell line (MCF-7)

All the synthesized compounds were evaluated for their antiproliferative effect on human breast carcinoma cell line MCF-7 at 100 $\mu\text{g}/\text{mL}$ utilizing MTT assay (**Fig.2**). The compounds which showed percentage of inhibition higher than 70% were further assessed for determination of median growth inhibitory concentration (IC_{50}) and doxorubicin was used as the standard drug as shown in **Table 1**. Moreover, the active compounds were also screened for their cytotoxic effects on human normal skin fibroblasts cell line BJ-1 at 100 $\mu\text{g}/\text{mL}$ (**Fig.3**).

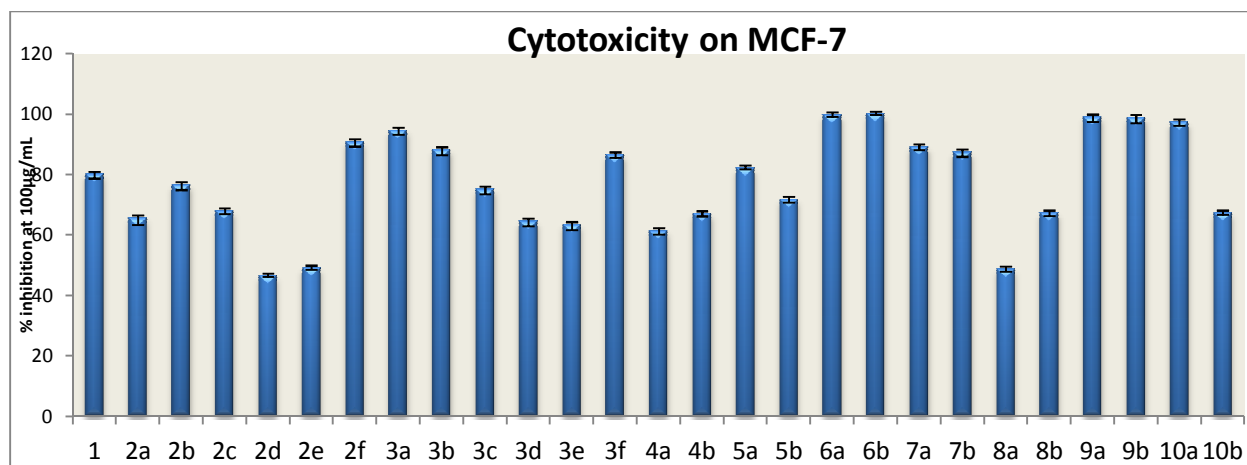


Fig.2. *In vitro* screening of the antiproliferative activities of compounds against human breast carcinoma cell line (MCF-7). Preliminary concentration for screening was 100µg/mL. Each result is a mean of 3 replicate samples and values are represented as % inhibition (\pm standard deviation)

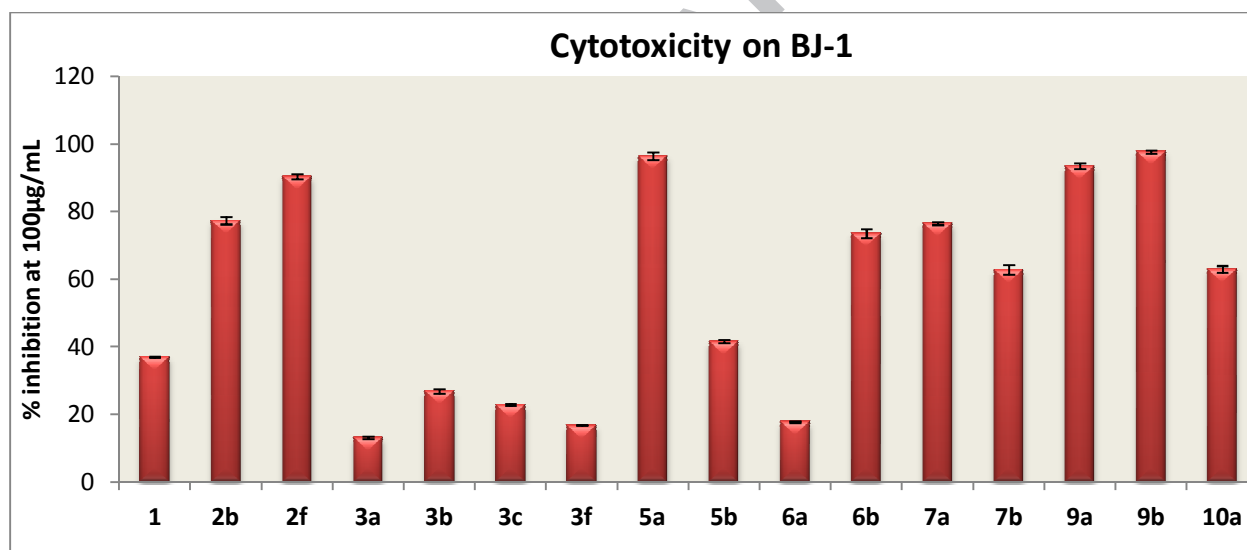


Fig.3. *In vitro* cytotoxic screening of the active compounds against human normal skin cell line (BJ-1). Preliminary concentration for screening was 100µg/mL. Each result is the mean of 3 replicate samples and values are represented as % inhibition (\pm standard deviation)

The results revealed that the tested compounds showed IC_{50} values ranging from 4.3-78 µg/mL compared to doxorubicin ($IC_{50} = 26.1$ µg/mL) towards MCF-7 cells. The 3,4,5-trimethoxyphenyl Schiff's base **2f**, phenyl thiazoles **7a** and **7b** and the thiazolidinones **3a**, **3b** and **3f** showed remarkably potent anticancer effects (IC_{50} values of 4.3, 9.3, 10.6, 11.1, 16.7 and

21.2 $\mu\text{g/mL}$, respectively), higher than the reference doxorubicin ($\text{IC}_{50} = 26.1 \mu\text{g/mL}$). On the other hand, compounds **1**, **6b** and **9a** showed comparable potency to that of the reference doxorubicin with IC_{50} values of 25.2, 28.0 and 30.6 $\mu\text{g/mL}$, respectively.

Table 1. IC_{50} of the active cytotoxic compounds exhibiting more than 70% cytotoxicity on MCF-7.

Compounds	IC_{50} ($\mu\text{g/mL}$)*
1	25.2 \pm 2.1
2b	38.1 \pm 3.2
2f	4.3 \pm 4.3
3a	11.1 \pm 1.9
3b	16.7 \pm 2.3
3c	42.0 \pm 4.8
3f	21.2 \pm 3.2
5a	36.9 \pm 1.4
5b	78.0 \pm 5.1
6a	42.0 \pm 4.4
6b	28.0 \pm 1.8
7a	9.3 \pm 4.2
7b	10.6 \pm 3.2
9a	30.6 \pm 1.3
9b	41.9 \pm 4.9
10a	37.0 \pm 3.5
doxorubicin	26.1 \pm 1.3

*Values of IC_{50} (\pm standard deviation) are calculated using SPSS statistical program.

Furthermore, it was obvious that the thiazolidinones **3a**, **3b** and **3f** with promising cytotoxic effect against MCF-7 revealed low cytotoxicity on normal BJ-1 cells with % inhibition= 13.2, 26.9 and 16.8%, respectively, which makes them interesting candidates for further biological evaluation (**Figure 3**).

2.2.2. Structure activity relationship

The 3,4,5-trimethoxyphenyl Schiff's base **2f** was the most active derivative among all the synthesized compounds with IC_{50} of 4.3 $\mu\text{g/mL}$. It showed higher anticancer effect than the parent hydrazide compound ($\text{IC}_{50} = 25.2 \mu\text{g/mL}$). In addition, the 3,4,5-trimethoxyphenyl Schiff's base **2f** displayed higher percentage of inhibition of MCF-7 than the 3,4-dimethoxyphenyl and the 4-methoxyphenyl derivatives **2e** and **2d** at 100 $\mu\text{g/mL}$ (% inhibition= 90.7, 48.9 and 46.3%, respectively). While the 4-chlorophenyl Schiff's base **2b** showed moderate anticancer potency ($\text{IC}_{50} = 38.1 \mu\text{g/mL}$), it displayed higher percentage of MCF-7 inhibition at 100 $\mu\text{g/mL}$ than the 4-

bromophenyl and 4-fluorophenyl congeners **2c** and **2a** (% inhibition= 76.5, 67.8 and 65.5%, respectively).

The 3,4,5-trimethoxyphenyl thiazolidinone compound **3f** showed lower anticancer effect than the parent Schiff's base **2f** (IC_{50} =21.2 μ g/mL). On the other hand the trimethoxyphenyl thiazolidinone **3f** displayed higher percentage of MCF-7 inhibition at 100 μ g/mL than the 3,4-dimethoxyphenyl and 4-methoxyphenyl derivatives **3e** and **3d** (% inhibition = 86.4, 63.3 and 64.4%, respectively). It could be observed that increasing the number of methoxy groups is parallel to improving the anticancer affect as explored by Schiff's bases **2d**, **2e** and **2f** and their cyclized thiazolidinone compounds **3d**, **3e** and **3f**. Cyclization of 4-halophenyl Schiff's bases into the corresponding thiazolidinones improved the anticancer effect. The 4-fluorophenyl thiazolidinone **3a** was the most active thiazolidinone compound with IC_{50} of 11.1 μ g/mL. It was more active than the 4-chlorophenyl derivative **3b** (IC_{50} = 17.7 μ g/mL) while a dramatic drop in the anticancer effect was displayed for the 4-bromophenyl thiazolidinone **3c** (IC_{50} = 42.0 μ g/mL).

Both *N*-methyl and *N*-ethyl derivatives of coumarinyl-4-phenylthiazoloacetohydrazides **7a** and **7b**, respectively, showed significant equipotent anticancer effect (IC_{50} = 9.3 and 10.6 μ g/mL, respectively) than the 4-methylthiazolyl congeners **5a** and **5b** (IC_{50} = 36.9 and 78 μ g/mL, respectively). On the other hand, the 5-acetyl-3-ethyl-4-methylthiazoline derivative **6b** showed higher anticancer potential against MCF-7 than the 3,4-dimethylthiazoline compound **6a** (IC_{50} = 28.0 and 42.0 μ g/mL, respectively). Generally the thiazolyl acetohydrazide derivatives **5a,b**, **6a,b** and **7a,b** were more potent than the oxothiazolidinyl acetohydrazides **8a** and **8b** and their parent thiosemicarbazide derivatives **4a** and **4b**.

Regarding the open chain derivatives, the *N*-methyl derivative of oxobutanoate and propanoate compounds **9a** and **10a** (IC_{50} = 30.6 and 37.0 μ g/mL, respectively) were more potent than its *N*-ethyl congeners **9b** (IC_{50} = 41.9 μ g/mL) and **10b** (% inhibition=67.1%).

2.2.3. *Tubulin polymerization inhibiting effect*

Among the common chemotherapeutic agents currently used in treating metastatic breast cancer are the antimetotics drugs.^{35,36} These agents bind primarily to β -tubulin, a major protein in the mitotic spindles causing a reduction in the dynamics of microtubules in the mitotic spindles, thus preventing spindle assembly and disturbing the normal movement of sister chromatids towards the spindle poles.³⁷⁻⁴⁰

Accordingly, in order to evaluate the role of tubulin beta polymerization (TUBb) on MCF-7 cells proliferation and to figure out the possible mode of action of the most cytotoxic and selective compounds towards MCF-7 cells, the tubulin beta polymerization inhibitory effect of the target compounds was assessed utilizing colchicine as a reference drug. This assay was performed for compounds **3a**, **3b** and **3f** which displayed the highest potential against MCF-7 cell line ($IC_{50} = 11.1, 16.7$ and $21.2 \mu\text{g/mL}$) with the least cytotoxicity on normal BJ-1 cells. Tubulin beta polymerization inhibiting effect of the target compounds **3a**, **3b** and **3f** was determined and IC_{50} values were calculated as summarized in **table 2**.

Table 2. Tubulin polymerization inhibiting effect of the target compounds.

Compound	IC_{50} (μM)
3a	9.37 ± 0.61
3b	2.89 ± 0.17
3f	6.13 ± 0.32
colchicine	6.93 ± 0.26

The three tested compounds showed significant TUBb polymerization inhibition activity in accordance with the *in vitro* cytotoxic activity against MCF-7 cell line. Compound **3b** showed outstanding TUBb polymerization inhibiting effect with IC_{50} value of $2.89 \mu\text{M}$. It was the most active TUBb polymerization inhibitor and was about 2.4 fold more active than the standard colchicine drug ($IC_{50} = 6.93 \mu\text{M}$). Compound **3f** was as potent inhibitor as colchicine with IC_{50} value of $6.13 \mu\text{M}$ and also compound **3a** showed remarkable TUBb polymerization inhibiting effect ($IC_{50} = 9.37 \mu\text{M}$). Although compound **3a** showed more cytotoxic effect against MCF-7 than **3b** and **3f**, it was not the most potent TUBb polymerization inhibitor which indicates that inhibiting tubulin polymerization is not the only way for its antitumor activity.

2.2.4. Cellular mechanism of action

2.2.4.1. Cell apoptosis

Based on the well-balanced cytotoxic activity and tubulin polymerization inhibition effect, compound **3a** which demonstrated the most potent and selective cytotoxic effect against MCF-7 cell line and exhibited significant inhibitory potency towards TUBb polymerization, was chosen for further investigation of its cellular mechanism of action regarding its effects on cell cycle progression and induction of apoptosis in MCF-7 cancer cells.

For evaluating the apoptosis process, flow cytometry was carried out using propidium iodide (PI) and annexinV-FITC in MCF-7 cells.⁴¹ After treatment with IC_{50} concentration of

compound **3a** (11.1 μ g/mL) for 24 hours, the cells were labeled with the two dyes. The corresponding red (PI) and green (FITC) fluorescence were detected with the flow cytometry. In comparison to DMSO as a negative control (**Fig. 4A**), it was observed that compound **3a** induced an increase in the late/secondary cellular apoptosis from 0.09% (DMSO control) to 10.63% (**Fig. 4B**). Also, an increase in the early/primary apoptosis was observed for compound **3a** of 5.49% (0.18% DMSO control). These data confirmed the apoptotic effect of compound **3a**.

2.2.4.2. Cell cycle arrest

To further elucidate the molecular mechanism by which compound **3a** exhibited its anti-proliferative activity against MCF-7 cells, its effect on cell cycle distribution was analyzed by flow cytometry.⁴¹ After exposure of MCF-7 cells to compound **3a** at 11.1 μ g/mL for 24 hours, it induced a significant increase in the percentage of cells at pre-G1 phase by 28.6 folds compared to control (**Fig. 4. C and D**). In addition, accumulation of cells was detected at G2/M phase by 5 folds compared to the control, from 8.59% in the vehicle group (**Fig. 4. C**) to 43.59 % in the group treated with the compound **3a** (**Fig. 4. D**). These results revealed that compound **3a** inhibited MCF-7 cells proliferation through the induction of G2/M phase arrest which led to cell cycle cessation at G2/M phase and prevented its mitotic cycle. These results are in agreement with the previously reported findings which investigated that the microtubule depolymerization pathway is well established and plays a crucial role in the G2/M phase arrest and induction of apoptosis.⁴²⁻⁴⁵

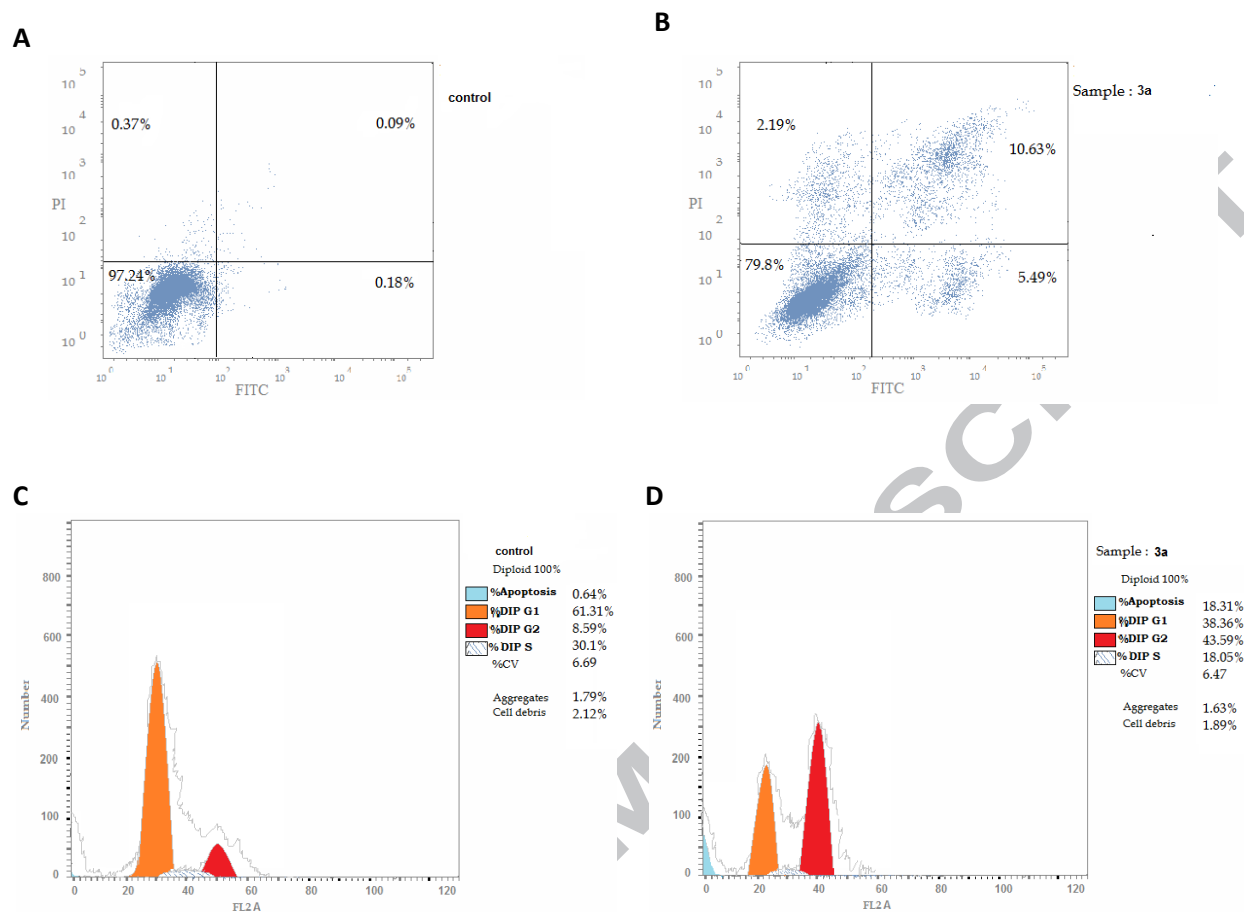


Fig.4. Cellular mechanism of action of compound **3a**. **(A, B)** Induction of apoptosis by compound **3a**. Cells were exposed to **3a** for 24h and analyzed by annexin V/ PI staining. The percentage of cells undergoing apoptosis is defined as the sum of early apoptotic (annexin V+/ PI-) cell percentage and late apoptotic (annexin V+/ PI+) cell percentage. **(C, D)** Cell cycle analysis of MCF-7 after incubation with compound **3a** for 24 h. DMSO diluent was used as a control.

2.2.4.3. Effect of compound 3a on the level of active caspase-7

Induction of apoptosis *via* either intrinsic (mitochondrial) or extrinsic (death receptor) pathways is mediated by caspase cascade events. Caspases are cysteine proteases which play an essential role in the initiation of apoptosis due to proapoptotic signals, so it could be considered that activating caspases is a significant step in apoptotic cell death.^{46,47} It has been demonstrated that inhibition of executing caspase 3 and/or 7 is crucial for the programmed cell death of multiple cell types.⁴⁸ Because MCF-7 cells lack endogenous caspase-3, the level of active

caspase-7 was assessed time-dependently in MCF-7 cells treated with compound **3a** at a concentration of 11.1 μ g/mL for 24 hours. As shown in **table 3**, treatment with compound **3a** resulted in significant increase in caspase-7 level compared to doxorubicin.

Table 3. Caspase-7 concentration in MCF-7 cells after treatment with compound **3a** for 24 hours.

Compound		Results	
Cpd.	Conc. μ g/mL	Casp7 conc. ng/mL	FLD
3a	11.1	1.162	3.236769
Doxorubicin	26.1	1.813	5.050139
Control		0.359	1

2.3. Molecular modeling studies

2.3.1. Molecular docking

In order to determine the possible binding modes of promising compounds **3a**, **3b** and **3f**, docking studies were carried out using the reported high-resolution crystal structure of the tubulin/DAMA-colchicine complex (PDB ID: 1SA0). Compounds **3a**, **3b** and **3f** were docked in the colchicine binding pocket using MOE software. The colchicine binding pocket is a deep pocket positioned at the α/β interface of tubulin heterodimer and consists of three zones, zone 1 located at α subunit interface, zone 2 which is the main zone situated at β subunit and most structures of colchicine binding site inhibitors occupied this zone, and zone 3 which is buried much deeper in β subunit.⁴⁹ Interaction mode of colchicine showed that cycloheptanone ring interacts with Ser α 178, Val α 181 and Val β 315 (zone 1) by van der Waals while, the carbonyl group forms H-bond with Val α 181 at a distance of 3.56 \AA . The trimethoxy phenyl group is embedded deeply in the hydrophobic portion of the pocket (zone 2) and surrounded by Leu β 242, Ala β 250, Lys β 254, Leu β 255, Ala β 316, Asn β 350, Lys β 352 and Ile β 378. The methoxy group behaves as H-bond acceptor and forms H-bond with thiol group of Cys241 at a distance of 3.31 \AA (**Fig. 5**). Binding mode of compound **3a** was nearly the same as that of colchicine and it mostly occupied zone 2 in a similar manner to the binding mode of colchicine inhibitors. Closure look to the docked pose of compound **3a** within colchicine pocket illustrates the following features: i) van der Waals interaction of oxothiazolidine acetamide with Ser α 178, Thr α 179 Ala α 180 and Val α 181 (zone1) in a similar manner to colchicine. ii) Carbonyl group of acetamide accepted two

hydrogen atoms, one from OH-Ser α 178 at a distance of 2.61Å and another one from OH - Threa179 at a distance of 2.82Å. Interestingly, the acetamide carbonyl group exhibited the same orientation of the carbonyl of cycloheptanone ring of colchicine (**Fig. 6 and 7**). iii) Coumarin moiety located at zone 2, likewise the trimethoxyphenyl group of colchicine, showed hydrophobic interactions with amino acids of zone 2 (Leu β 242, Ala β 250, Lys β 254, Leu β 255, Ala β 316 and Lys β 352). iv) Carbonyl group of coumarin moiety formed H-bond with NH of Val β 318 at a distance of 3.33Å. In addition, the 4-phenyl group linked to coumarin was embedded deeply in the hydrophobic pocket in zone 2 facing Cys β 241.

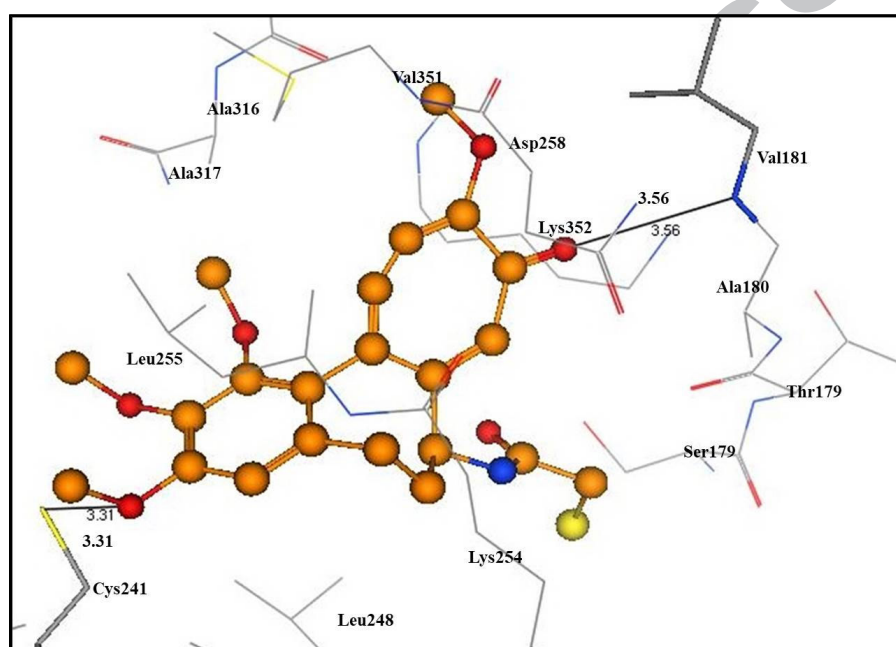


Fig.5. The binding mode and molecular interactions of co-crystallized ligand; colchicine. Color code: ligand (orange, ball) and black-line as hydrogen-bond interactions between residues and ligand

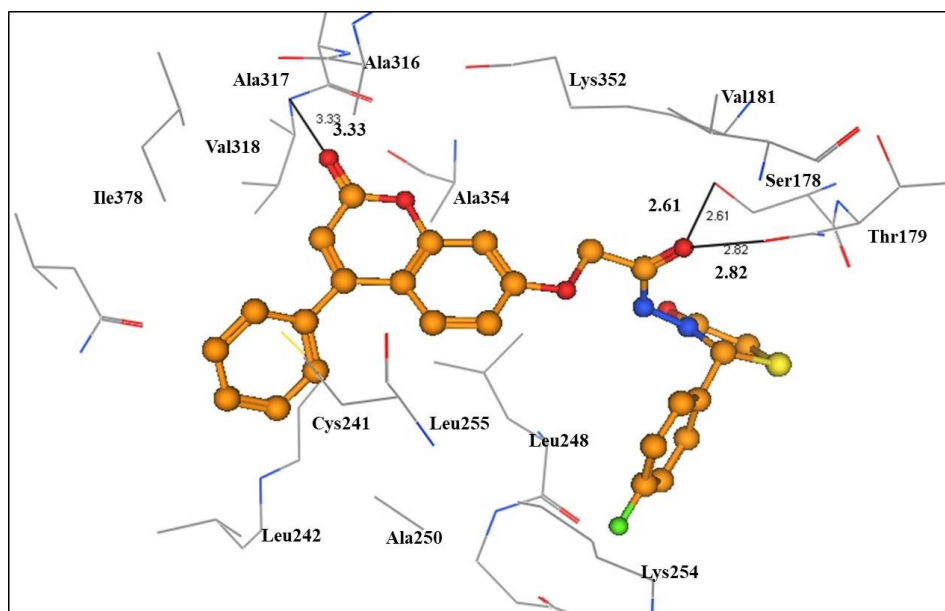


Fig.6. molecular interactions of compound **3a** (orange, ball), within the colchicine binding site, hydrogen-bonds are represented as black-line, C=O of acetamide formed two H-bonds with Ser178 and Thr179. C=O of coumarin formed H-bond with Val318.

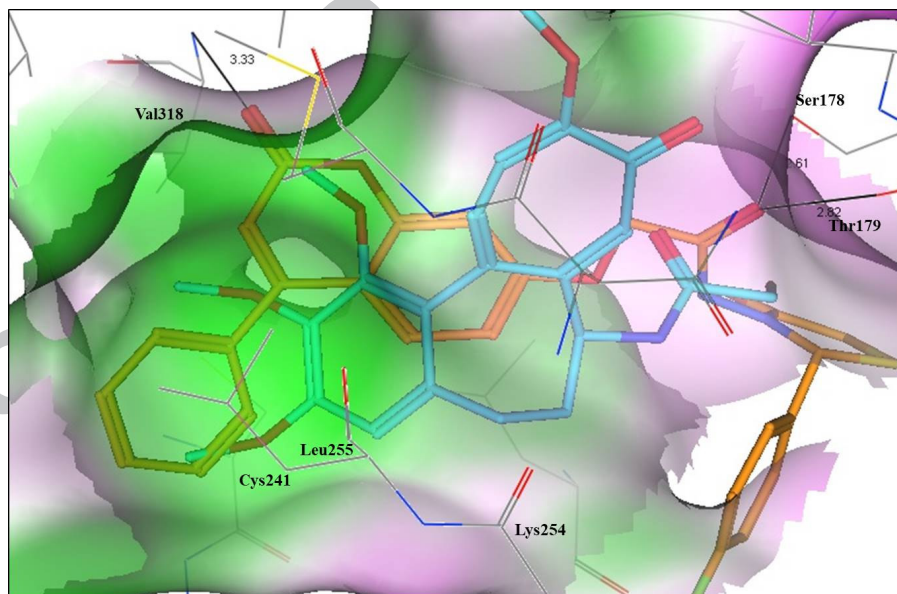


Fig.7. The binding mode of compound **3a** (orange, stick) within the active site of tubulin protein (PDB:1SA0), showed that coumarin moiety located at zone 2, in similar manner to trimethoxyphenyl group of colchicine (blue, stick), both C=O group of acetamide of compound **3a** and C=O group of colchicine showed the same orientation. The binding surface code colour, white; neutral, pink; hydrophilic, green; hydrophobic.

Docking results of compound **3b** showed that i) 4-Chlorophenyl thiazolidinone moiety showed hydrophobic interactions with zone 1 amino acids (Ser α 178, Thr α 179 and Val α 181). ii) Carbonyl group of oxothiazolidine received H atom from NH-Asn α 101 and formed H-bond at a distance of 2.56Å. in addition, carbonyl group of acetamide formed another H-bond with NH of Lys β 254 at a distance of 2.70Å. Third H-bond was formed between C=O of coumarin and NH-Ala β 354 at a distance of 3.68Å. iii) Coumarin moiety buried in the hydrophobic portion of the pocket was restricted with residues of zone 2 (Leu β 242, Ala β 250, Lys β 254, Leu β 255 and Lys β 352), additionally, phenyl group linked to coumarin moiety of compound **3b** was embedded deeply within the hydrophobic region of zone 2 in contact with Cys β 241 (Fig.8 and 9).

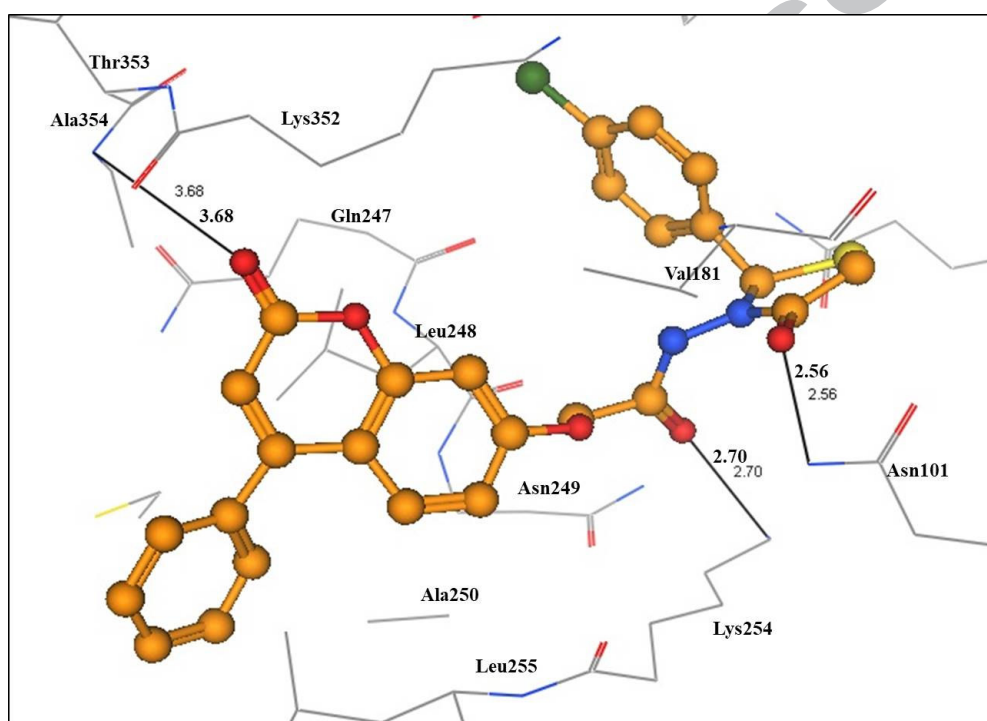


Fig.8. Molecular interactions of compound **3b** (orange, ball), at the colchicine binding site. C=O moiety formed H-bond with Asn α 101, C=O acetamide formed H-bond with Lys β 254 and C=O coumarin formed H-bond with Ala β 354. Hydrogen-bond interactions between residues and ligand are represented as black lines.

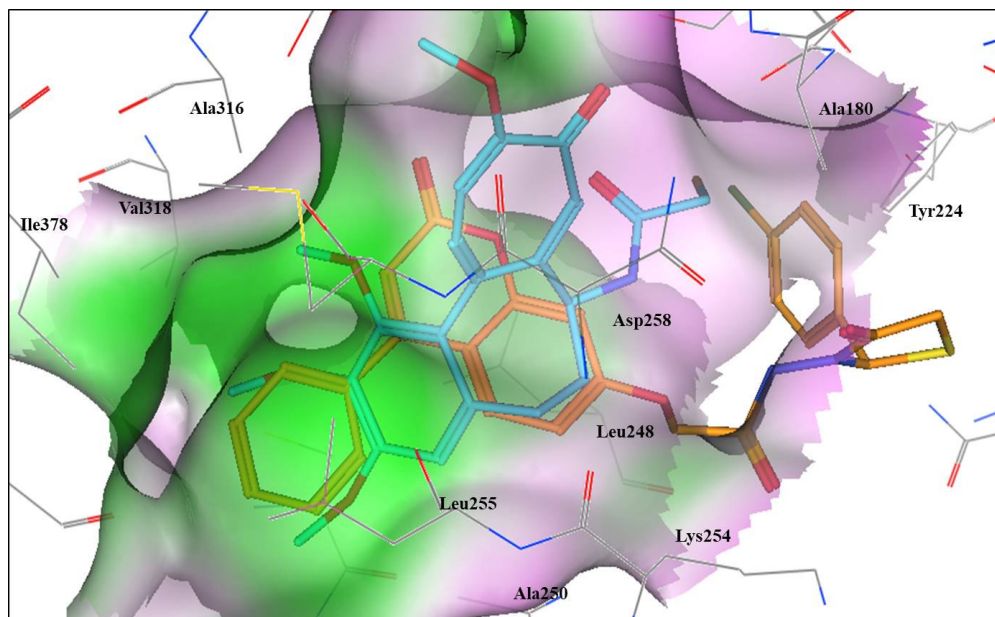


Fig 9. The binding mode of compound **3b** (orange, stick). Coumarin moiety was buried in the hydrophobic portion of the pocket restricted with residues of zone 2, in similar manner to trimethoxy phenyl of colchicine (blue, stick).

Binding mode of compound **3f** is highly similar to compounds **3a** and **3b**, as the same interaction features were found i) Trimethoxy phenyl thiazolidinone moiety showed the same hydrophobic interaction with zone 1 amino acids (Ser α 178 and Thr α 179). ii) Carbonyl group of acetamide formed two H- bonds with OH-Ser α 178 at a distance of 2.61Å and with OH - Thr α 179 at a distance of 2.86Å. The acetamide carbonyl group of compound **3f** exhibited the same orientation of the carbonyl group of colchicine cycloheptenone ring. iii) Carbonyl moiety of coumarin received H atom from NH-Val β 318 and formed H-bond at a distance of 3.27Å. Also, coumarin moiety showed the same hydrophobic interactions with zone 2 amino acids ((Leu β 242, Ala β 250, Lys β 254, Leu β 255, Ala β 316, Lys β 352 and Ile378). Finally, the 4-phenyl group linked to coumarin moiety showed the same position within the hydrophobic pocket of colchicine pocket site as in compounds **3a** and **3b** (**Fig.10** and **11**).

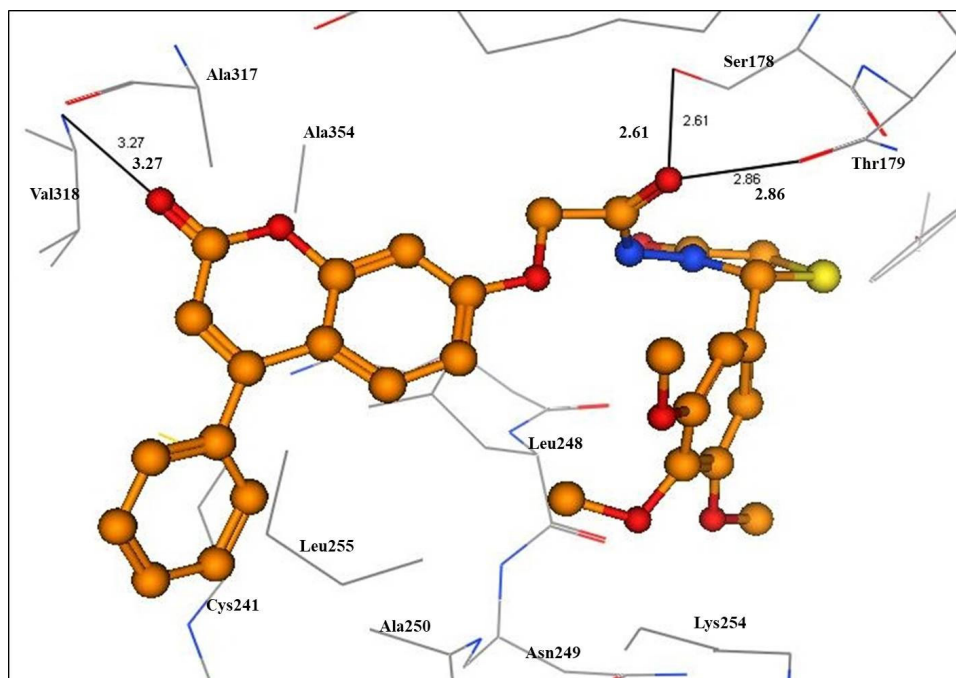


Fig.10. Molecular interactions of compound **3f** (orange, ball) within the colchicine binding site, C=O acetamide formed two H-bonds with Ser α 178 and Thr α 179. C=O coumarin formed H-bond with Val β 318. Colour code: Hydrogen-bond interactions between residues and ligand are represented as black lines.

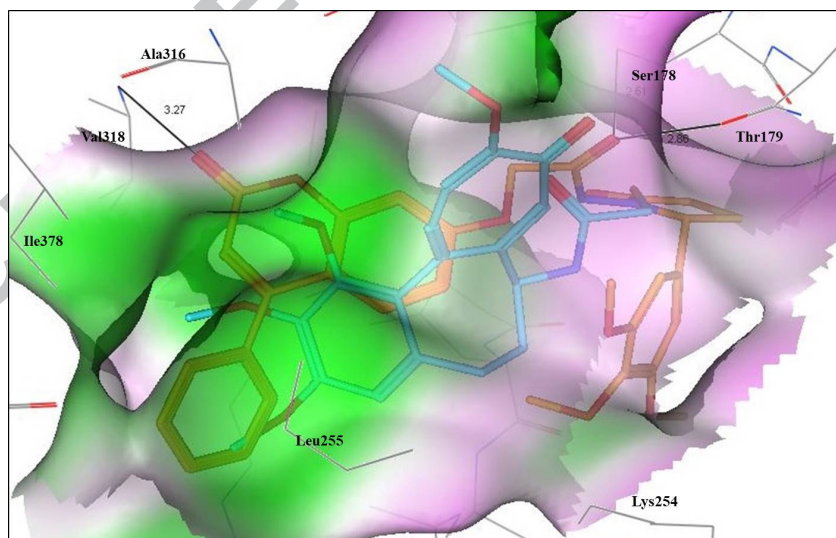


Fig.11. The binding mode of compound **3f** (orange, stick) showed that coumarin moiety located at zone 2, in similar manner to trimethoxy phenyl group of colchicine (blue, stick), both C=O group of acetamide of compound **3f** and C=O group of colchicine showed the same orientation.

In conclusion, the three compounds **3a**, **3b** and **3f** showed the same binding mode within the colchicine binding site, which is similar to colchicine. The thiazolidinone moiety showed two types of interactions, hydrophobic interactions and H-bond formation between carbonyl group of oxothiazolidine and amino acids of zone 1, these interactions are similar to that of cycloheptanone moiety of colchicine. In addition, coumarin moiety of the three compounds illustrated hydrophobic interactions with amino acids of zone 2 (important zone for colchicine inhibitors). Besides, the H-bonds were formed between the C=O groups of the three compounds and zone 2 residues. It is noticeable that these molecular interactions are the common interactions of colchicine inhibitors, which explain the inhibition activity of compounds **3a**, **3b** and **3f**.

2.3.2. Pharmacophores

Nguyen *et al.*,⁴⁹ identified the common pharmacophore model of colchicine binding inhibitors which consists of seven pharmacophore points: i) Three H-bond acceptors, A1 in contact with Val β 181, A2 in contact with Cys β 241, and A3 establishing one contact mainly with Ala β 250, Asp β 251, and Leu β 252. ii) One hydrogen bond donor, D1, which interacts with Thr β 179. iii) Two hydrophobic centers, H1 and H2. iv) A planar group R1. It should be noted that, none of the colchicine binding inhibitors possessed all the 7-points of pharmacophore.⁵⁰ With the aim of rationalizing the key common binding interactions of compounds **3a**, **3b** and **3f**, the pharmacophore hypotheses for these compounds were built and compared with Nguyen's model. Pharmacophore hypothesis of compound **3a** (**Fig.12A**) showed four features, two hydrogen bond acceptors (HBA) F1 in contact with Ser α 178 and Thr α 179 and F2 in contact with Val β 318 and two hydrophobic centers F3 in contact with Leu β 248, Ala β 250, Leu β 255 and Ala β 345 and F4 which showed hydrophobic interactions with Cys β 241 and Leu β 255. Compound **3b** pharmacophore hypothesis showed five features, three H-bonds acceptors represented by carbonyl groups of oxothiazolidine, acetamide and coumarin moieties, in addition to two hydrophobic centers made up by coumarin moiety and phenyl group (**Fig.12B**). Compound **3f** pharmacophore model illustrated the same four features as compound **3a** (**Fig.12C**). It is clear from the results of the three pharmacophore models that there is an agreement with Nguyen's pharmacophore model, as the three pharmacophores showed four points common with the points

identified by Nguyen. Furthermore, there is a good correspondence between the pharmacophore points and the docking results.

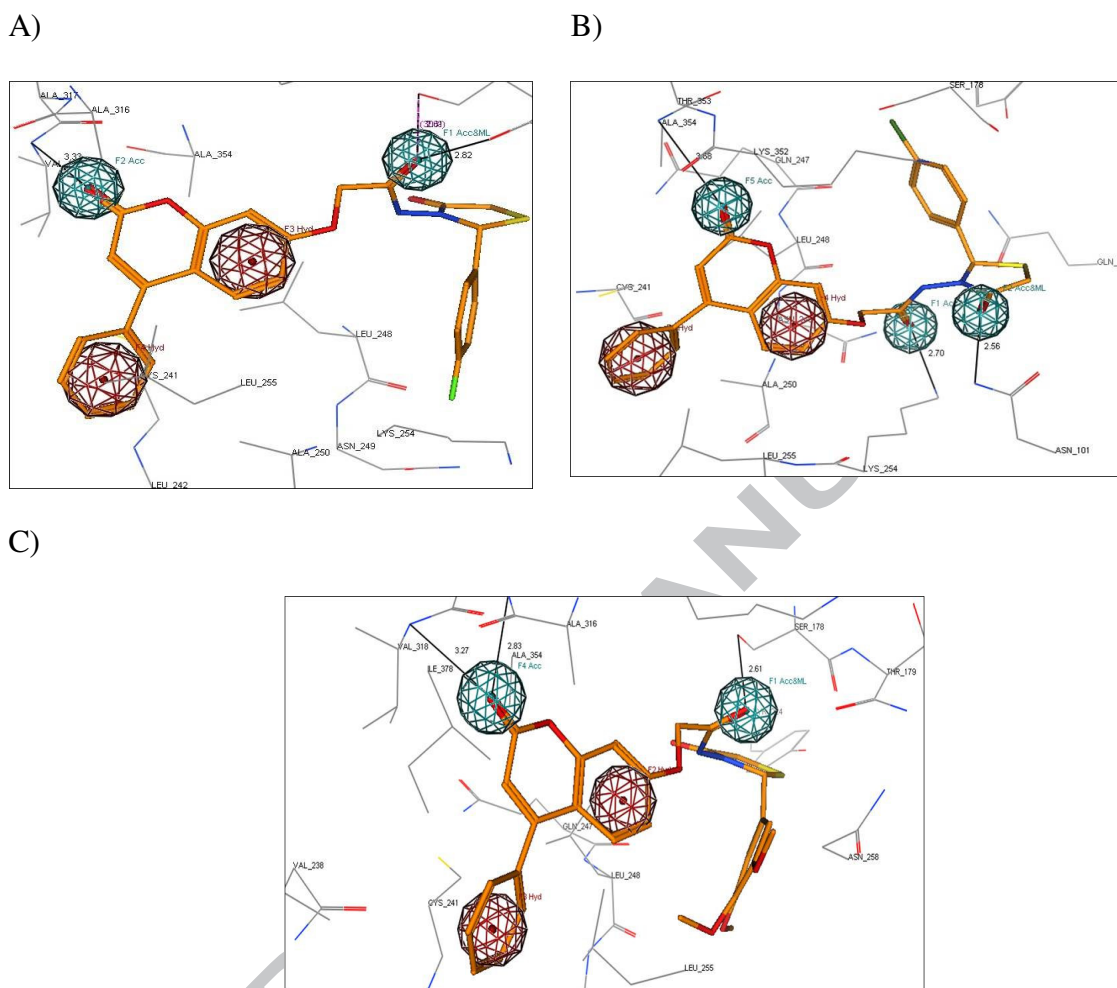


Fig. 12. Pharmacophore models include hydrogen bond acceptors centres (dark blue), hydrophobic centres (dark red). **A)** Represented compound **3a** with 4 features. **B)** Represented compound **3b** with 5 features. **C)** represented compound **3f** with 4 features

2.3.3. Molecular dynamics studies (MD)

In order to study the stability of the docked poses produced by the molecular docking studies and investigate their binding modes within colchicine binding site, compounds **3a**, **3b** and **3f** were subjected to MD studies. The ligand–receptor complexes of **3a**, **3b** and **3f** that came out from the docking simulation were used in the MD simulation study for 100 picoseconds (Ps). It was noticeable from the study of the root mean square deviation (RMSD) of compound **3a** that, the compound fluctuated in the first 30Ps. Starting from the 35Ps, the compound become

stable and the complex (protein-ligand) reached the stable state and the average RMSD of compound **3a** during the simulation was 3Å which is a small distance indicating the effectiveness and the strength of H-bonds between the ligand and protein (**Fig.13 A**). Compound **3b**–protein complex fluctuated in the first 25 Ps then became stable starting from the 25Ps. In the Ps 45-55, compound **3a** dropped down then retained the steady state for the remaining of the simulation (**Fig.13 B**). Molecular dynamics simulation of compound **3f** reached the balance after the 25Ps, and RMSD of compound **3f** was kept around a small distance of 1 Å (**Fig.13 C**).

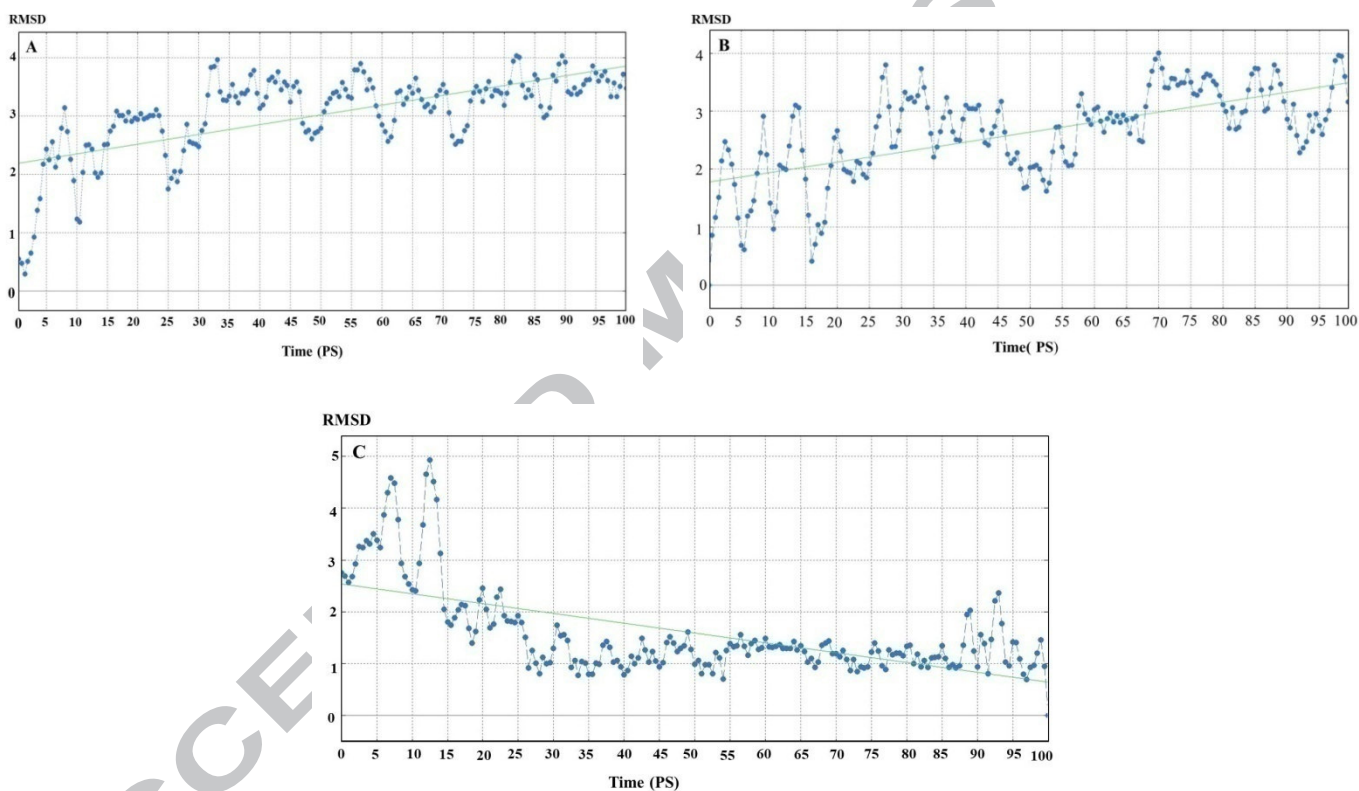


Fig.13. **A)** Molecular dynamic simulation of compound **3a** showed RMSD (Å) over 100Ps. **B)** Molecular dynamic simulation of compound **3b** showed the RMSD (Å) over 100Ps. **C)** Molecular Dynamic simulation of compound **3f** showed RMSD (Å) over 100Ps.

2.3.4. Energy study

Potential and kinetic energies in Kcal/mol were calculated for compound **3a** during the MD simulation, the analysis of potential energy graph showed that the potential energy of the system was so high in the first 10Ps, and the pattern reached the steady state at 25 Ps with

potential energy equal to 150 Kcal/mol (**Fig. 14A**). Kinetic energy figure of compound **3a** fluctuated in the first 25 Ps and it was so high in the first 10 Ps. The equilibrium was reached at 25Ps in a similar manner to the potential energy (**Fig. 14B**). The RMSD result of compound **3a** showed that compound **3a** got stable after 30Ps. i.e. after the system reached to potential and kinetic energy equilibrium as proved by potential and kinetic energy results which indicated the reliability of MD results.

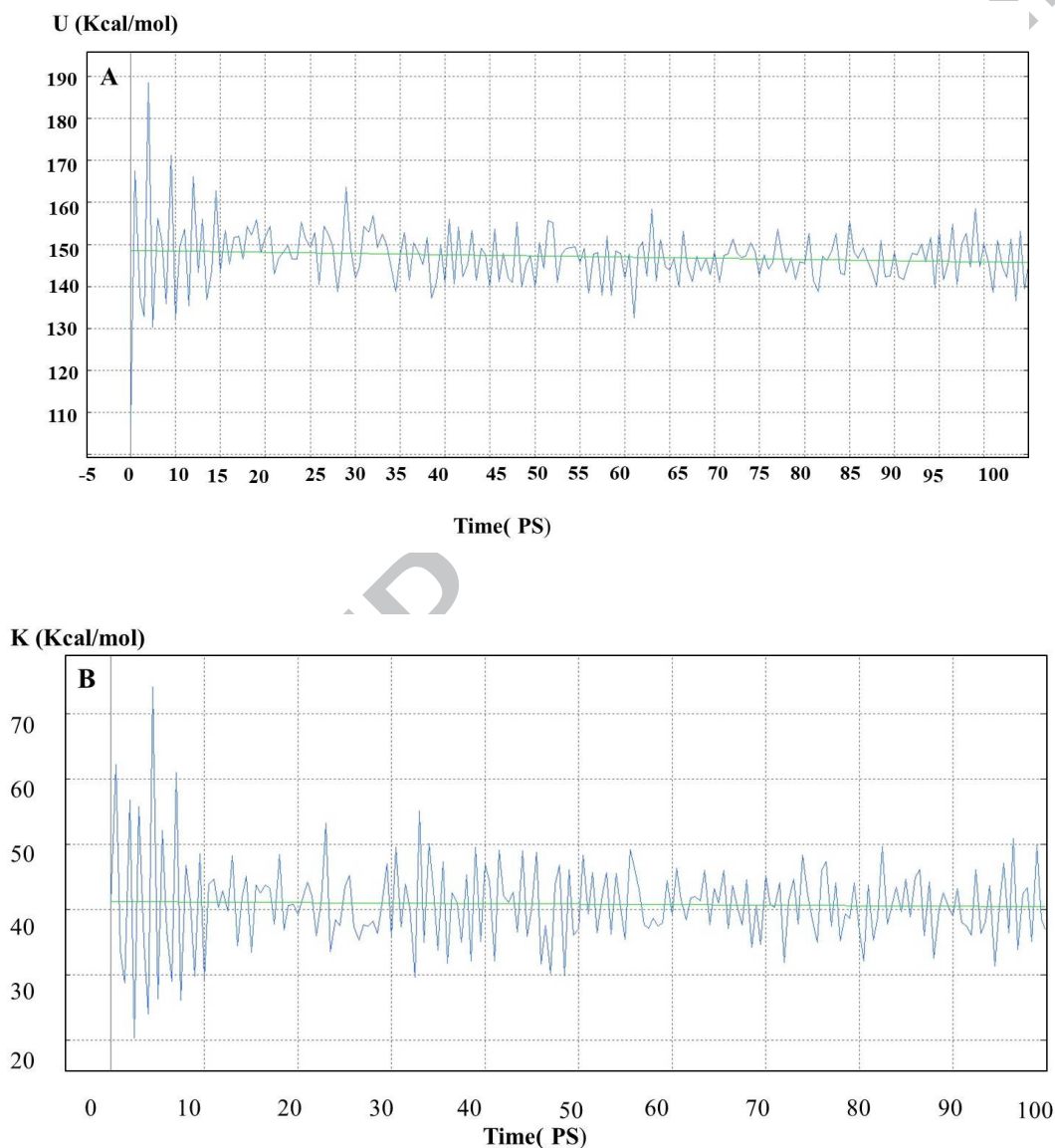


Fig14. **A)** Molecular dynamic simulation of compound **3a** showed the potential energy (Kcal/mol) over 100Ps. **B)** Molecular dynamic simulation of compound **3a** showed the Kinetic energy(Kcal/mol) over 100Ps.

2.3.5. Molecular property-based drug-likeness rules

Lipinski proposed the “Rule of Five”,⁵¹ the most popular drug-likeness filter, which provides four rules to determine whether a molecule is well orally absorbed or not: octanol/water partition coefficient ($\log P$) ≤ 5 , molecular weight (MW) ≤ 500 , number of hydrogen bond acceptors (HBA) ≤ 10 and number of hydrogen bond donors (HBD) ≤ 5 . In this study the four rules were calculated for compound **3a**. In addition, polar surface area (PSA) was also calculated, as it is thought that compounds with promising oral bioavailability have PSA ≤ 140 Å.⁵² Calculated molecular property of compound **3a** based on drug likeness rules showed that compound **3a** fulfilled Lipinski rule, as $\log P = 5$, Mwt = 490, number of hydrogen bond acceptor (HBA) = 4, number of hydrogen bond donors (HBD) = 1 and PSA = 84.9 (**Table 4**), this indicates that compound **3a** is well orally absorbed

In a similar manner to the purpose of Lipinski rules, the REOS (Rapid Elimination of Swill) program was developed at Vertex,⁵³ the drug-likeness criteria that are developed by REOS include six rules: MW (200 ~ 500), number of hydrogen bond donors (0 ~ 5), number of hydrogen bond acceptors (0 ~ 10), $\log P$ (-5 ~ 5), number of rotatable bonds (0 ~ 8) and number of formal charge (-2 ~ 2). Calculated number of rotatable bonds and formal charge for compound **3a** were; 7 and 0 respectively, this reveals that compound **3a** obeys REOS rules. These results confirm the oral bioavailability of our promising compound **3a** (**Table 4**).

Table 4. The calculated Lipinski and REOS criteria for compound **3a**.

Compound	Parameters						
	Mwt	HBA	HBD	$\log P$	Rotatable bonds	Formal charge	PSA
3a	490	4	1	5	7	0	84.9

3. Conclusion

In this study, new 4-phenylcoumarin derivatives were developed for cytotoxic assessment against human breast cancer cell line MCF-7. Cytotoxic effect of the synthesized compounds against MCF-7 revealed that most of the compounds showed promising antiproliferative effects against MCF-7. Compounds **3a**, **3b** and **3f** displayed remarkable cytotoxic effect on MCF-7 with no significant cytotoxic effect on human normal skin cell line (BJ-1). Furthermore, tubulin

polymerization assay was performed for the most promising and selective cytotoxic compounds **3a**, **3b** and **3f**. The results disclosed that the three derivatives demonstrated equal to higher inhibitory potency of TUBb polymerization when compared to the reference drug colchicine of IC_{50} values ($IC_{50} = 9.37, 2.89$ and $6.13 \mu\text{M}$, respectively, vs $6.93 \mu\text{M}$ for colchicine). Compound **3a** was further subjected to cellular mechanistic studies on MCF-7 cells and revealed induction of apoptosis and cell cycle arrest at G2/M phase, along with its significant activation of caspase-7 that might mediate apoptosis of MCF-7 cancer cells. The combined analyses of molecular docking, pharmacophore hypotheses and MD studies revealed significant information on the structural features of the promising molecules, which are required for interactions and afforded a guide for the design of novel lead compounds. Molecular modeling studies showed that compounds **3a**, **3b** and **3f** had the same binding mode of colchicine. In addition, molecular modeling and pharmacophore models displayed that the most important features of interactions are the carbonyl groups of thiazolidinone, acetamide and coumarin moieties, in addition to two hydrophobic centers made up by coumarin moiety and phenyl group. MD illustrated that compound **3a**-complex became stable at 30Ps with very low RMSD value, also compounds **3b** and **3f** reached the stable state at 25Ps with low RMSD value. MD results supported the reliability of docking studies. Lipinski's rule calculations showed that all the physical and pharmacokinetic properties of compound **3a** are within the accepted range indicating that compound **3a** is promising as drug like molecule.

4. Experimental

4.1. Chemistry

All melting points were uncorrected and measured using Electrothermal IA 9000 apparatus. Infrared spectra were measured by Nexus 670 FT-IR FT-Raman spectrometer using KBr discs at National Research Centre, Egypt. The nuclear magnetic resonance NMR spectra were determined utilizing Varian mercury 300 MHz spectrometer and using TMS as the internal standard. The mass spectra were recorded on GCMS-QP 1000EX Shimadzu Gas Chromatography MS Spectrometer. ^1H NMR, ^{13}C NMR, EI-MS and the elemental analyses were performed at Micro-Analytical Laboratory, Central Services Laboratory, Faculty of Science, Cairo University, Egypt. The reactions were followed by TLC (silica gel, aluminum sheets 60 F254, Merck) using chloroform-methanol (9.5:0.5 v/v) as eluent and sprayed with iodine-potassium iodide reagent. The purity of the newly synthesized compounds was assessed by TLC

and elemental analysis and was found to be higher than 95%. Compounds **1,2b**, **2d**, **3b** and **3d** were previously prepared.⁵⁴

4.1.1. General procedure for the preparation of Schiff's bases 2a-f

To a mixture of the hydrazide compound **1** (3.1g, 0.01 mol) in absolute ethanol (20 ml) containing glacial acetic acid (5mL), different aromatic aldehydes (0.01 mol), namely; 4-fluorobenzaldehyde (1.07mL), 4-chlorobenzaldehyde (1.41g), 4-bromobenzaldehyde (1.85 g), 4-methoxybenzaldehyde (1.22 mL), 3,4-dimethoxybenzaldehyde (1.66g) and / or 3,4,5-trimethoxybenzaldehyde (1.96 g) were added. The reaction mixture was refluxed for 6-8 hours. The formed precipitate was filtered off and re-crystallized from acetic acid to afford the title compounds.

2-(2-Oxo-4-phenyl-2H-chromen-7-yloxy)-N'-(4-fluorobenzylidene)acetohydrazide 2a

Yield 75%, mp 260-2°C. Anal. Calcd. for C₂₄H₁₇FN₂O₄ (416.4): C, 69.23; H, 4.12; N, 6.73. Found: C, 69.36; H, 4.23; N, 6.89. IR (cm⁻¹, KBr): 3210 (NH), 1719 (C=O), 1688 (C=O). ¹HNMR (DMSO-*d*₆, δ, ppm): 5.80 (2H, s, OCH₂), 6.26 (1H, s, H-3 coumarin), 6.88-7.58 (12H, m, Ar-H), 8.26 (1H, s, N=CH), 11.66 (1H, s, NH, D₂O exchangeable). MS (EI, 70eV) *m/z* (%): 416 (M⁺) (16.8 %), 293 (100.00%).

2-(2-Oxo-4-phenyl-2H-chromen-7-yloxy)-N'-(4-bromobenzylidene)acetohydrazide 2c

Yield 85%, mp 271-2°C. Anal. Calcd. for C₂₄H₁₇BrN₂O₄ (477.31): C, 60.39; H, 3.59; N, 5.87. Found: C, 60.26; H, 3.42; N, 5.69. IR (cm⁻¹, KBr): 3211 (NH), 1715(C=O), 1689 (C=O). ¹HNMR (DMSO-*d*₆, δ, ppm): 5.72 (2H, s, OCH₂), 6.26 (1H, s, H-3 coumarin), 6.90-7.57 (12H, m, Ar-H), 8.23 (1H, s, N=CH), 11.69 (1H, s, NH, D₂O exchangeable). MS (EI, 70eV) *m/z* (%): 477,479 (M⁺, M⁺+2) (14.83, 14.11 %), 295 (100.00%).

2-(2-Oxo-4-phenyl-2H-chromen-7-yloxy)-N'-(3,4-dimethoxybenzylidene)acetohydrazide 2e

Yield 80%, mp 238-40°C. Anal. Calcd. for C₂₆H₂₂N₂O₆ (458.46): C, 68.11; H, 4.84; N, 6.11. Found: C, 68.27; H, 4.98; N, 6.26. IR (cm⁻¹, KBr): 3210 (NH), 1720 (C=O), 1686 (C=O). ¹HNMR (DMSO-*d*₆, δ, ppm): 3.70 (3H, s, OCH₃), 3.72 (3H, s, OCH₃), 5.76 (2H, s, OCH₂), 6.26 (1H, s, H-3 coumarin), 6.92-7.58 (11H, m, Ar-H), 8.24 (1H, s, N=CH), 11.41 (1H, s, NH, D₂O exchangeable). MS (EI, 70eV) *m/z* (%): 458 (M⁺) (13.9 %), 193 (100.00%).

2-(2-Oxo-4-phenyl-2H-chromen-7-yloxy)-N'-(3,4,5-trimethoxybenzylidene)acetohydrazide 2f

Yield 85%, mp 204-6°C. Anal. Calcd. for C₂₇H₂₄N₂O₇ (488.49): C, 66.39; H, 4.95; N, 5.73. Found: C, 66.26; H, 4.82; N, 5.59. IR (cm⁻¹, KBr): 3212 (NH), 1718 (C=O), 1684 (C=O).

^1H NMR (DMSO- d_6 , δ , ppm): 3.62 (3H, s, OCH₃), 3.75 (6H, s, 2OCH₃), 5.77 (2H, s, OCH₂), 6.25 (1H, s, H-3 coumarin), 6.72-7.55 (10H, m, Ar-H), 8.23 (1H, s, N=CH), 11.49 (1H, s, NH, D₂O exchangeable). MS (EI, 70eV) m/z (%): 488 (M⁺) (100.00%).

4.1.2. General procedure for the preparation of thiazolidinone compounds 3a-f

Thioglycolic acid (0.001 mol, 0.07 mL) was added to a well stirred solution of Schiff's bases **2a-f** (0.001 mol) in dry benzene (20 mL) and the reaction mixture was refluxed for 7-9 hours. After completion of the reaction, excess solvent was evaporated under reduced pressure and the residue was neutralized with cold dilute sodium bicarbonate solution, the formed product was filtered off, washed with water and then re-crystallized from acetic acid to give the thiazolidinone compounds **3a-f**.

2-(2-Oxo-4-phenyl-2H-chromen-7-yloxy)-N-(2-(4-fluorophenyl)-4-oxothiazolidin-3-yl)acetamide 3a

Yield 65%, mp 198-200°C. Anal. Calcd. for C₂₆H₁₉FN₂O₅S (490.5): C, 63.66; H, 3.90; N, 5.71; S, 6.54. Found: C, 63.56; H, 3.78; N, 5.59; S, 6.43. IR (cm⁻¹, KBr): 3177 (NH), 1719 (C=O), 1683 (C=O), 1624 (C=O). ^1H NMR (DMSO- d_6 , δ , ppm): 3.74-3.95 (2H, dd, CH₂ thiazolidinone), 4.71 (2H, s, OCH₂), 5.82 (1H, s, CH thiazolidinone), 6.27 (1H, s, H-3 coumarin), 6.90-7.59 (12H, m, Ar-H), 10.54 (1H, s, NH, D₂O exchangeable). MS (EI, 70eV) m/z (%): 490 (M⁺) (1.74%), 165 (100.00%).

2-(2-Oxo-4-phenyl-2H-chromen-7-yloxy)-N-(2-(4-bromophenyl)-4-oxothiazolidin-3-yl)acetamide 3c

Yield 67%, mp 230-2°C. Anal. Calcd. for C₂₆H₁₉BrN₂O₅S (551.41): C, 56.63; H, 3.47; N, 5.08; S, 5.82. Found: C, 56.49; H, 3.38; N, 4.91; S, 5.73. IR (cm⁻¹, KBr): 3182 (NH), 1717 (C=O), 1685 (C=O), 1623 (C=O). ^1H NMR (DMSO- d_6 , δ , ppm): 3.75-3.94 (2H, dd, CH₂ thiazolidinone), 4.72 (2H, s, OCH₂), 5.79 (1H, s, CH thiazolidinone), 6.27 (1H, s, H-3 coumarin), 6.93-7.58 (12H, m, Ar-H), 10.54 (1H, s, NH, D₂O exchangeable). ^{13}C NMR (DMSO- d_6 , δ , ppm): 29.01, 60.88, 65.84, 101.98, 111.73, 112.55, 120.54, 122.02, 127.61, 128.15, 128.26, 128.74, 129.53, 129.80, 131.31, 134.82, 137.50, 154.84, 155.02, 159.70, 160.43, 166.06, 168.52. MS (EI, 70eV) m/z (%): 551, 553 (M⁺, M⁺+2) (0.50, 0.50%), 295 (100.00%).

2-(2-Oxo-4-phenyl-2H-chromen-7-yloxy)-N-(2-(3,4-dimethoxyphenyl)-4-oxothiazolidin-3-yl)acetamide 3e

Yield 70%, mp 135-7°C. Anal. Calcd. for C₂₈H₂₄N₂O₇S (532.56): C, 63.15; H, 4.54; N, 5.26; S, 6.02. Found: C, 63.27; H, 4.68; N, 5.37; S, 6.11. IR (cm⁻¹, KBr): 3179 (NH), 1719 (C=O), 1689 (C=O), 1628 (C=O). ¹HNMR (DMSO-*d*₆, δ, ppm): 3.70 (3H, s, OCH₃), 3.72 (3H, s, OCH₃), 3.75-3.89 (2H, dd, CH₂ thiazolidinone), 4.72 (2H, s, OCH₂), 5.77 (1H, s, CH thiazolidinone), 6.26 (1H, s, H-3 coumarin), 6.82-7.58 (11H, m, Ar-H), 10.48 (1H, s, NH, D₂O exchangeable). MS (EI, 70eV) *m/z* (%): 532 (M⁺) (1.47 %), 182 (100.00%).

2-(2-Oxo-4-phenyl-2H-chromen-7-yloxy)-N-(2-(3,4,5-trimethoxyphenyl)-4-oxothiazolidin-3-yl)acetamide 3f

Yield 71%, mp 150-2°C. Anal. Calcd. for C₂₉H₂₆N₂O₈S (562.59): C, 61.91; H, 4.66; N, 4.98; S, 5.70. Found: C, 61.79; H, 4.52; N, 4.87; S, 5.61. IR (cm⁻¹, KBr): 3183 (NH), 1716 (C=O), 1688 (C=O), 1625 (C=O). ¹HNMR (DMSO-*d*₆, δ, ppm): 3.62 (3H, s, OCH₃), 3.75 (6H, s, 2OCH₃), 3.77-3.91 (2H, dd, CH₂ thiazolidinone), 4.75 (2H, s, OCH₂), 5.78 (1H, s, CH thiazolidinone), 6.25 (1H, s, H-3 coumarin), 6.73-7.59 (10H, m, Ar-H), 10.51 (1H, s, NH, D₂O exchangeable). MS (EI, 70eV) *m/z* (%): 562 (M⁺) (4.41 %), 59 (100.00%).

4.1.3. General Procedure for the preparation of 1-(2-(2-oxo-4-phenyl-2H-chromen-7-yloxy)acetyl)-4-methyl and / or ethylthiosemicarbazide 4a,b.

To a solution of the hydrazide **1** (3.1g, 0.01 mol) in hot absolute ethanol, methyl isothiocyanate (0.68 mL, 0.01mol) and/or ethyl isothiocyanate (0.87g, 0.01mol) was added. The mixture was refluxed for 5-7 hours and the separated solid was filtered, washed with ethanol and crystallized from acetic acid.

1-(2-(2-Oxo-4-phenyl-2H-chromen-7-yloxy)acetyl)-4-methylthiosemicarbazide 4a.

Yield 85%, mp 217-9°C. Anal. Calcd. for C₁₉H₁₇N₃O₄S (383.42): C, 59.52; H, 4.47; N, 10.96; S, 8.36. Found: C, 59.64; H, 4.63; N, 11.19; S, 8.48. IR (cm⁻¹, KBr): 3399, 3376, 3310 (3NH), 1702 (C=O), 1670 (C=O). ¹HNMR (DMSO-*d*₆, δ, ppm): 2.88-2.89 (3H, d, CH₃), 4.74 (2H, s, OCH₂), 6.26 (1H, s, H-3 coumarin), 6.81-7.57 (8H, m, Ar-H), 7.83-7.85 (1H, q, NHCH₃, D₂O exchangeable), 10.18 (1H, s, NH, D₂O exchangeable), 13.91(1H, s, NH, D₂O exchangeable). MS (EI, 70eV) *m/z* (%): 383 (M⁺) (13%), 163 (100%).

1-(2-(2-Oxo-4-phenyl-2H-chromen-7-yloxy)acetyl)-4-ethylthiosemicarbazide 4b.

Yield 80%, mp 219-21°C. Anal. Calcd. for C₂₀H₁₉N₃O₄S (397.45): C, 60.44; H, 4.82; N, 10.57; S, 8.07. Found: C, 60.34; H, 4.71; N, 10.49; S, 7.91. IR (cm⁻¹, KBr): 3385, 3376, 3325, (3NH), 1708 (C=O), 1675 (C=O). ¹HNMR (DMSO-*d*₆, δ, ppm): 1.05-1.09 (3H, t, CH₃), 3.47-3.49 (2H,

m, CH₂), 4.73 (2H, s, OCH₂), 6.26 (1H, s, H-3 coumarin), 6.99–7.57 (8H, m, Ar–H), 7.99–8.02 (1H, t, NHCH₂, D₂O exchangeable), 9.19 (1H, s, NH, D₂O exchangeable), 10.08 (1H, s, NH, D₂O exchangeable). MS (EI, 70eV) *m/z* (%): 397 (M⁺) (3%), 161 (100%).

4.1.4. General Procedure for the preparation of 2-(2-oxo-4-phenyl-2H-chromen-7-yloxy)-N'-(3,4-dialkylthiazol-2(3H)-ylidene)acetohydrazide (5a,b), 2-(2-oxo-4-phenyl-2H-chromen-7-yloxy)-N'-(5-acetyl-3,4-dialkylthiazol-2(3H)-ylidene) acetohydrazide (6a,b) and 2-(2-Oxo-4-phenyl-2H-chromen-7-yloxy)-N'-(3-alkyl-4-phenylthiazol-2(3H)-ylidene)acetohydrazide (7a,b).

A mixture of compounds **4a,b** (0.01 mol) and the appropriate α -halocarbonyl compounds (0.01mol), namely, chloroacetone (0.82 mL), 3-chloroacetylacetone (1.13 mL) and / or phenacyl bromide (1.99 g), in absolute ethanol (30 mL) containing sodium acetate anhydrous (1.64 g, 0.02 mol) was refluxed for 10-12 hours. After cooling the precipitate was filtered, washed with water, dried, and re-crystallized from absolute ethanol to give compounds **5a,b**, **6a,b** and **7a,b**, respectively.

2-(2-Oxo-4-phenyl-2H-chromen-7-yloxy)-N'-(3,4-dimethylthiazol-2(3H)-ylidene) acetohydrazide 5a

Yield 70%, mp 106–8°C. Anal. Calcd. for C₂₂H₁₉N₃O₄S (421.47): C, 62.69; H, 4.54; N, 9.97; S, 7.61. Found: C, 62.50; H, 4.39; N, 9.82; S, 7.51. IR (cm⁻¹, KBr): 3465, (NH), 1713 (C=O), 1646 (C=O). ¹HNMR (DMSO-*d*₆, δ , ppm): 2.24 (3H, s, CH₃), 3.61 (3H, s, N-CH₃), 4.26 (2H, s, OCH₂), 6.28 (1H, s, H-3 coumarin), 7.06–7.56 (10H, m, Ar–H, S-CH and NH). MS (EI, 70eV) *m/z* (%): 421 (M⁺) (12.06 %), 184 (100.00%).

2-(2-Oxo-4-phenyl-2H-chromen-7-yloxy)-N'-(3-ethyl-4-methylthiazol-2(3H)-ylidene) acetohydrazide 5b

Yield 75%, mp 80–2°C. Anal. Calcd. for C₂₃H₂₁N₃O₄S (435.5): C, 63.43; H, 4.86; N, 9.65; S, 7.36. Found: C, 63.59; H, 4.99; N, 9.83; S, 7.50. IR (cm⁻¹, KBr): 3452, (NH), 1711 (C=O), 1641 (C=O). ¹HNMR (DMSO-*d*₆, δ , ppm): 1.05–1.08 (3H, t, CH₃-CH₂), 2.25 (3H, s, CH₃), 4.02–4.06 (2H, q, CH₂-CH₃), 4.29 (2H, s, OCH₂), 6.27 (1H, s, H-3 coumarin), 6.98–7.56 (10H, m, Ar–H, S-CH and NH). MS (EI, 70eV) *m/z* (%): 435 (M⁺) (5.85 %), 57 (100.00%).

2-(2-oxo-4-phenyl-2H-chromen-7-yloxy)-N'-(5-acetyl-3,4-dimethylthiazol-2(3H)-ylidene) acetohydrazide 6a

Yield 82%, mp 123-5°C. Anal. Calcd. for C₂₄H₂₁N₃O₅S (463.51): C, 62.19; H, 4.57; N, 9.07; S, 6.92. Found: C, 62.29; H, 4.72; N, 9.19; S, 7.08. IR (cm⁻¹, KBr): 3420 (NH), 1700 (C=O), 1682 (C=O), 1614 (C=O). ¹HNMR (DMSO-*d*₆, δ, ppm): 1.63 (3H, s, CH₃ thiazole), 2.24 (3H, s, COCH₃), 3.61 (3H, s, NCH₃), 4.26 (2H, s, OCH₂), 6.27 (1H, s, H-3 coumarin), 7.03–7.57 (9H, m, Ar–H and NH). MS (EI, 70eV) *m/z* (%): 464 (M⁺+1) (1.73%), 238 (100.00%).

2-(2-oxo-4-phenyl-2H-chromen-7-yloxy)-N'-(5-acetyl-3-ethyl-4-methylthiazol-2(3H)-ylidene) acetohydrazide 6b

Yield 80%, mp 122-4°C. Anal. Calcd. for C₂₅H₂₃N₃O₅S (477.53): C, 62.88; H, 4.85; N, 8.80; S, 6.71. Found: C, 63.01; H, 4.97; N, 8.98; S, 6.88. IR (cm⁻¹, KBr): 3422, (NH), 1703 (C=O), 1680 (C=O), 1614 (C=O). ¹HNMR (DMSO-*d*₆, δ, ppm): 1.30-1.32 (3H, t, CH₃-CH₂), 1.67 (3H, s, CH₃ thiazole), 2.25 (3H, s, COCH₃), 4.02-4.06 (2H, q, CH₂-CH₃), 4.30 (2H, s, OCH₂), 6.26 (1H, s, H-3 coumarin), 7.29–7.58 (9H, m, Ar–H and NH). MS (EI, 70eV) *m/z* (%): 477(M⁺) (1.36 %), 57 (100.00%).

2-(2-Oxo-4-phenyl-2H-chromen-7-yloxy)-N'-(3-methyl-4-phenylthiazol-2(3H)-ylidene) acetohydrazide 7a

Yield 80%, mp 170-2°C. Anal. Calcd. for C₂₇H₂₁N₃O₄S (483.54): C, 67.07; H, 4.38; N, 8.69; S, 6.63. Found: C, 67.19; H, 4.49; N, 8.83; S, 6.81. IR (cm⁻¹, KBr): 3432, (NH), 1724 (C=O), 1680 (C=O). ¹HNMR (DMSO-*d*₆, δ, ppm): 3.63 (3H, s, N-CH₃), 4.93 (2H, s, OCH₂), 6.28 (1H, s, H-3 coumarin), 7.03–8.02 (15H, m, Ar–H, S-CH and NH). MS (EI, 70eV) *m/z* (%): 483 (M⁺) (7.92%), 105 (100.00%).

2-(2-Oxo-4-phenyl-2H-chromen-7-yloxy)-N'-(3-ethyl-4-phenylthiazol-2(3H)-ylidene) acetohydrazide 7b

Yield 85%, mp 178-80°C. Anal. Calcd. for C₂₈H₂₃N₃O₄S (497.56): C, 67.59; H, 4.66; N, 8.45; S, 6.44. Found: C, 67.77; H, 4.79; N, 8.63; S, 6.55. IR (cm⁻¹, KBr): 3433, (NH), 1726 (C=O), 1681 (C=O). ¹HNMR (DMSO-*d*₆, δ, ppm): 1.29-1.34 (3H, t, CH₃-CH₂), 4.05-4.11 (2H, q, CH₂-CH₃), 4.98 (2H, s, OCH₂), 6.27 (1H, s, H-3 coumarin), 7.02–8.03 (15H, m, Ar–H, S-CH and NH). MS (EI, 70eV) *m/z* (%): 497 (M⁺) (1.19%), 105(100.00%).

4.1.5. General procedure for the synthesis of 2-(2-oxo-4-phenyl-2H-chromen-7-yloxy)-N'-(3-methyl/ and or ethyl-4-oxothiazolidin-2-ylidene) acetohydrazides 8a,b

A mixture of the thiosemicarbazides **4a,b** (0.01 mol), ethylbromoacetate (0.01 mol, 1.11 mL) and sodium acetate anhydrous (0.02 mol, 1.64 g) in absolute ethanol (30 mL) was refluxed

for 8-10 hours. After cooling the precipitate was filtered, washed with water, dried, and recrystallized from absolute ethanol to give compounds **8a,b**.

2-(2-Oxo-4-phenyl-2H-chromen-7-yloxy)-N'-(3-methyl-4-oxothiazolidin-2-ylidene) acetohydrazide 8a

Yield 85%, mp 259-60°C. Anal. Calcd. for C₂₁H₁₇N₃O₅S (423.44): C, 59.57; H, 4.05; N, 9.92; S, 7.57. Found: C, 59.77; H, 4.22; N, 10.17; S, 7.71. IR (cm⁻¹, KBr): 3281 (NH), 1715 (C=O), 1682 (C=O), 1615 (C=O). ¹HNMR (DMSO-*d*₆, δ, ppm): 3.62 (3H, s, N-CH₃), 4.06 (2H, s, S-CH₂, thiazolidinone), 5.45 (2H, s, OCH₂), 6.28 (1H, s, H-3 coumarin), 7.06–7.57 (8H, m, Ar-H), 10.58 (1H, s, NH, D₂O exchangeable). MS (EI, 70eV) *m/z* (%): 423 (M⁺) (84.85 %), 158 (100.00%).

2-(2-Oxo-4-phenyl-2H-chromen-7-yloxy)-N'-(3-ethyl-4-oxothiazolidin-2-ylidene) acetohydrazide 8b

Yield 82%, mp 212-4°C. Anal. Calcd. for C₂₂H₁₉N₃O₅S (437.47): C, 60.40; H, 4.38; N, 9.61; S, 7.33. Found: C, 60.57; H, 4.52; N, 9.77; S, 7.51. IR (cm⁻¹, KBr): 3264 (NH), 1717 (C=O), 1683 (C=O), 1616 (C=O). ¹HNMR (DMSO-*d*₆, δ, ppm): 1.11-1.16 (3H, t, CH₃-CH₂), 3.66-3.73 (2H, q, CH₂-CH₃), 4.05 (2H, s, S-CH₂, thiazolidinone), 4.79 (2H, s, OCH₂), 6.26 (1H, s, H-3 coumarin), 6.98–7.57 (8H, m, Ar-H), 10.58 (1H, s, NH, D₂O exchangeable). ¹³C NMR (DMSO-*d*₆, δ ppm): 11.94, 32.60, 37.41, 66.39, 101.95, 111.54, 112.72, 120.40, 120.45, 127.72, 128.27, 128.74, 129.53, 134.86, 154.96, 155.15, 159.75, 160.97, 163.12, 171.01. MS (EI, 70eV) *m/z* (%): 437 (M⁺) (12.08 %), 59 (100.00%).

4.1.6. General procedures for the preparation of ethyl-2-((N-methyl/ethyl-N'-(2-((2-oxo-4-phenyl-2H-chromen-7-yl)oxy)acetyl)carbamo hydrazonoyl)thio)-3-oxobutanoate 9a,b

A mixture of compounds **4a,b** (0.01mol), ethyl-2-chloroacetoacetate (0.01mol, 1.4mL) in absolute ethanol (30 mL) containing sodium acetate anhydrous (1.64 g, 0.02 mol) was refluxed for 8-10 hours. After cooling the precipitate was filtered, washed with water, dried, and recrystallized from absolute ethanol to give compounds **9a,b**.

Ethyl-2-((N-methyl-N'-(2-((2-oxo-4-phenyl-2H-chromen-7-yl)oxy)acetyl)carbamo hydrazonoyl)thio)-3-oxobutanoate 9a

Yield 80%, mp 155-7°C. Anal. Calcd. for C₂₅H₂₅N₃O₇S (511.55): C, 58.70; H, 4.93; N, 8.21; S, 6.27. Found: C, 58.87; H, 5.02; N, 8.37; S, 6.41. IR (cm⁻¹, KBr): 3421, 3264 (2NH), 1735 (C=O)

1728 (C=O), 1683 (C=O), 1616 (C=O). ¹HNMR (DMSO-*d*₆, δ, ppm): 1.12-1.17 (3H, t, CH₃-CH₂), 2.49 (3H, s, COCH₃), 3.61 (3H, s, NCH₃), 4.04-4.11 (2H, q, CH₂-CH₃), 4.06 (1H, s, S-CH), 5.45 (2H, s, OCH₂), 6.28 (1H, s, H-3 coumarin), 7.02-7.58 (10H, m, Ar-H and 2NH). ¹³C NMR (DMSO-*d*₆, δ ppm): 13.93, 30.50, 34.59, 60.56, 61.29, 102.53, 107.19, 111.89, 112.61, 113.04, 120.85, 120.93, 127.96, 128.46, 128.92, 129.74, 134.93, 151.55, 155.06, 155.27, 159.89, 160.63, 168.21. MS (EI, 70eV) *m/z* (%): 513(M⁺+2) (0.2 %), 59 (100.00%).

Ethyl-2-((N-ethyl-N'-(2-((2-oxo-4-phenyl-2H-chromen-7-yl)oxy)acetyl)carbamoyl)thio)-3-oxobutanoate 9b

Yield 85%, mp 144-6°C. Anal. Calcd. for C₂₆H₂₇N₃O₇S (525.57): C, 59.42; H, 5.18; N, 8.00; S, 6.10. Found: C, 59.60; H, 5.32; N, 8.17; S, 6.22. IR (cm⁻¹, KBr): 3428, 3263 (2NH), 1736 (C=O) 1728 (C=O), 1684 (C=O), 1615 (C=O). ¹HNMR (DMSO-*d*₆, δ, ppm): 1.13-1.17 (3H, t, CH₃-CH₂), 1.27-1.32 (3H, t, CH₃-CH₂), 2.49 (3H, s, COCH₃), 4.02-4.06 (2H, q, CH₂-CH₃), 4.07-4.10 (2H, q, CH₂-CH₃), 4.12 (1H, s, S-CH), 5.46 (2H, s, OCH₂), 6.27 (1H, s, H-3 coumarin), 7.02-7.58 (10H, m, Ar-H and 2NH). MS (EI, 70eV) *m/z* (%): 525(M⁺) (0.1 %), 59 (100.00%).

4.1.7. General procedures for the preparation of ethyl-2-((N-methyl/ ethyl-N'-(2-((2-oxo-4-phenyl-2H-chromen-7-yl)oxy)acetyl)carbamoyl)thio) propanoate 10a,b

A mixture of compounds **4a,b** (0.01mol), ethyl-2-bromopropionate (0.01mol, 1.3mL) in absolute ethanol (30 mL) containing sodium acetate anhydrous (1.64 g, 0.02 mol) was refluxed for 8-10 hours. After cooling the precipitate was filtered, washed with water, dried, and recrystallized from absolute ethanol to give compounds **10a,b**.

Ethyl-2-((N-methyl-N'-(2-((2-oxo-4-phenyl-2H-chromen-7-yl)oxy)acetyl)carbamoyl)thio)propanoate 10a

Yield 90%, mp 142-4°C. Anal. Calcd. for C₂₄H₂₅N₃O₆S (483.54): C, 59.61; H, 5.21; N, 8.69; S, 6.63. Found: C, 59.81; H, 5.32; N, 8.82; S, 6.81. IR (cm⁻¹, KBr): 3422, 3260 (2NH), 1732 (C=O), 1682 (C=O), 1615 (C=O). ¹HNMR (DMSO-*d*₆, δ, ppm): 1.08-1.12 (3H, t, CH₃-CH₂), 1.46-1.48 (3H, d, CH₃CH), 3.64 (3H, s, NCH₃), 3.99-4.07 (2H, q, CH₂CH₃), 4.16-4.22 (1H, q, CHCH₃), 5.47 (2H, s, OCH₂), 6.28 (1H, s, H-3 coumarin), 7.02-7.58 (10H, m, Ar-H and 2NH). ¹³C NMR (DMSO-*d*₆, δ ppm): 13.60, 17.34, 30.54, 44.20, 60.58, 61.06, 102.40, 111.74, 112.50, 112.85, 127.79, 128.25, 128.73, 129.54, 134.78, 148.69, 151.65, 154.88, 155.12, 159.67, 160.49, 170.67. MS (EI, 70eV) *m/z* (%): 483 (M⁺) (0.2 %), 59 (100.00%).

Ethyl-2-((N-ethyl-N'-(2-((2-oxo-4-phenyl-2H-chromen-7-yl)oxy)acetyl)carbamoylthio)propanoate 10b

Yield 92%, mp 157-9°C. Anal. Calcd. for C₂₅H₂₇N₃O₆S (497.56): C, 60.35; H, 5.47; N, 8.45; S, 6.44. Found: C, 60.54; H, 5.62; N, 8.63; S, 6.61. IR (cm⁻¹, KBr): 3428, 3265 (2NH), 1731 (C=O), 1681 (C=O), 1614 (C=O). ¹HNMR (DMSO-*d*₆, δ, ppm): 1.07-1.12 (3H, t, CH₃-CH₂), 1.25-1.30 (3H, t, CH₃-CH₂), 1.50-1.53 (3H, d, CH₃CH), 4.01-4.11 (3H, m, NCH₂CH₃ and CHCH₃), 4.27-4.30 (2H, q, OCH₂CH₃), 5.48 (2H, s, OCH₂), 6.28 (1H, s, H-3 coumarin), 7.01-7.58 (10H, m, Ar-H and 2NH). MS (EI, 70eV) *m/z* (%): 497 (M⁺) (0.3 %), 59 (100.00%).

4.2. Biology

4.2.1. *In vitro* anticancer MTT assay

The cytotoxicity of the newly synthesized compounds against cancer cell lines *in vitro* was performed by MTT assay.⁵⁵ The MTT assay is based on the reduction of the soluble 3-(4,5-dimethyl-2-thiazolyl)-2,5-diphenyl-2H-tetrazolium bromide (MTT) into a blue-purple formazan product, mainly by mitochondrial reductase activity inside the living cells.

4.2.1.1. Cell lines

Human breast carcinoma MCF-7 cell line and BJ-1 "A telomerase immortalized normal foreskin fibroblast cell line" were obtained from Karolinska Center, Department of Oncology and Pathology, Karolinska Institute and Hospital, Stockholm, Sweden.

4.2.1.2. Cell culture

The procedure was done in a sterile area using a laminar air flow cabinet biosafety class II level. Culture was maintained in DMEM F12 medium with 1% antibiotic-antimycotic mixture (10,000 U/ml potassium penicillin, 10,000 µg/ml streptomycin sulfate and 25µg/ml amphotericin B), 1% L-glutamine, and supplemented with 10% heat inactivated fetal bovine serum. Culturing and subculturing were carried out according to Thabrew *et al.*⁵⁶ Doxorubicin was used as a positive control. A negative control composed of DMSO was also used.

4.2.1.3. Cell viability assay

Following culturing for 10 days, the cells were seeded at concentration of 10x10³ cells per well in case of MCF-7 and 40-50 x10³ cells per well in case of BJ-1 in a fresh complete growth medium using 96-well microtiter plastic plates at 37 °C for 24 hours under 5% CO₂, in a water jacketed carbon dioxide incubator. Fresh medium (without serum) was added and cells were incubated either alone (negative control) or with samples to give a final concentration of

100µg/ml. After 24 hours incubation, the medium was aspirated and then 40µl MTT salt (2.5mg/ml) were added to each well and incubated for further four hours at 37°C under 5% CO₂. To stop the reaction and dissolve the formed crystals, 200µl 10% sodium dodecyl sulphate (SDS) in deionized water was added to each well and incubated overnight at 37°C. The absorbance was measured using a microplate multi-well reader at 595nm and a reference wavelength of 690nm. Cell viability was assessed according to the mitochondrial dependent reduction of yellow MTT (3-(4, 5-dimethylthiazol-2-yl)-2, 5-diphenyltetrazolium bromide) to purple formazan. The results were expressed as the IC₅₀ (µg/mL), which inducing a 50% inhibition of cell growth of the treated cells when compared to the growth of control cells. Each experiment was performed at least 3 times.⁵⁷

4.2.1.4. Determination of IC₅₀ values

IC₅₀ values were calculated for the promising active compounds possessing ≥ 70 % cytotoxicity using probit analysis and utilizing the SPSS computer program (SPSS for windows, statistical analysis software package /version 9/ 1989 SPSS Inc., Chicago, USA).

4.2.2. Enzyme-linked immunosorbent assay for tubulin beta (TUBb)

MCF-7 cells were cultured using DMEM (supplemented with 10% FBS and 1% penicillin-streptomycin. Plate cells (cells density 1.2 – 1.8 × 10,000 cells/well) in a volume of 100µL complete growth medium and 100 µL of the tested compound per well in a 96-well plate for 18–24 hours before the enzyme assay for Tubulin . The microtiter plate provided in this kit has been pre-coated with an antibody specific to TUBb. Standards or samples are then added to the appropriate microtiter plate wells with a biotin-conjugated antibody specific to TUBb. Next, Avidin conjugated to Horseradish Peroxidase (HRP) is added to each microplate well and incubated. After TMB substrate solution is added, only those wells that contain TUBb, biotin-conjugated antibody and enzyme-conjugated Avidin will exhibit a change in color. The enzyme-substrate reaction is terminated by the addition of sulphuric acid solution and the color change is measured spectrophotometrically at a wavelength of 450 nm ± 10 nm. The concentration of TUBb in the samples is then determined by comparing the O.D. of the samples to the standard curve.⁵⁸

4.2.3. Cell cycle analysis and apoptosis detection

Cell cycle analysis and apoptosis detection were carried out by flow cytometry. MCF-7 cells were seeded at 8 × 10⁴ and incubated at 37° C , 5% CO₂ overnight, After treatment with the

tested compound **3a**, for 24 hours, cell pellets were collected and centrifuged (300× g, 5 minutes). For cell cycle analysis, cell pellets were fixed with 70% ethanol on ice for 15 minutes and collected again.⁴¹ The collected pellets were incubated with propidium iodide (PI) staining solution at room temperature for 1 hour. Apoptosis detection was performed by Annexin V-FITC apoptosis detection kit (BioVision, Inc, Milpitas, CA, USA) following the manufacturer's protocol. The samples were analyzed using FACS Calibur flow cytometer (BD Biosciences, San Jose, CA).

4.2.4. Caspase-7 assay

Activities of caspase-7 were measured using Human CASP7 (Caspase 7) ELISA Kit from MyBioSource INC. Catalog # MBS2505226 (96 tests) (MyBioSource, Inc., San Diego, CA, USA) according to the manufacturer instructions.

4.3. Molecular modeling

4.3.1. Target preparation

The crystal structure of tubulin complex with DAMA-colchicine was retrieved from the RCSB Protein Data Bank (PDB ID: 1SA0, <http://www.rcsb.org>) and was selected as a target in the modeling study. Water molecules were deleted, hydrogen atoms were added and the energy of the system was minimized with MOE 2008.10 (Molecular Operating Environment, <http://www.chemcomp.com>).

4.3.2. Ligand preparation

The compounds were prepared with MOE 2008.10. Ligand structures were built with MOE and the energy was minimized, the placement criteria was chosen to be the MMFF94x force field until RMSD gradient of 0.05 kcal mol⁻¹ Å⁻¹ was reached.

4.3.3. Molecular docking

Compounds **3a**, **3b** and **3f** were docked within the colchicine binding site of the tubulin protein. The site of docking was considered using crystallographic ligand position and the important two zones of the interaction were identified. The placement criterion was adjusted to be Triangle Matcher. Rescoring 1 was selected to be London G and Retain 30 poses. In our study we prefer to make refinement with Force field and rescoring 2 was chosen to be London G.

4.3.4. Pharmacophore generation

The pharmacophore was built for the tubulin protein structure (PDB: 1SA0), using The Protein Ligand Interaction Fingerprints; PLIF statistical tool for analysis interactions of **3a**, **3b**

and **3f** with colchicine binding site. Pharmacophore query was used to create the pharmacophore features. The features were neither permissive nor excessively restrictive; the scheme of annotation was selected to be "Unified"

4.3.5. *Molecular dynamics (MD)*

MD were carried for compounds **3a**, **3b** and **3f** using the docked pose as the starting point and the analyses were performed with MOE; 2008.10 software. Partial charges were calculated for the system and energy minimizations were done, MD was carried for 100 Ps. Ensemble was selected to be NVT (N is the number of particles, V is the volume and T is the temperature). The relationship between Root mean square deviation (RMSD) and the time for the three compounds were calculated. The potential energy and kinetic energy for compound **3a** were calculated and their changes over 100 Ps were studied.

Acknowledgments

The authors extend their appreciation and thanking to Dr. Essam Rashwan, head of confirmatory diagnostic unit, Vacsera-Egypt, for helping in performing the tubulin polymerization, apoptosis and cell cycle arrest assays.

References:

1. Mitchison T, Kirschner M. Dynamic instability of microtubule growth. *Nature* 1984; 312: 237-42.
2. Bonnet C, Boucher D, Lazereg, S, Pedrotti B, Islam K, Denoulet P, Larcher J C. Differential binding regulation of microtubule-associated proteins MAP1A, MAP1B, and MAP2 by tubulin polyglutamylation. *J Biol Chem* 2001; 276: 12839-48.
3. Devred F, Tsvetkov P O, Barbier P, Allegro D, Horwitz S B, Makarov A A, Peyrot V. Stathmin/Op18 is a novel mediator of vinblastine activity. *FEBS Lett* 2008; 582: 2484-8.
4. Barbier P, Dorléans A, Devred F, Sanz L, Allegro D, Alfonso C, Knossow M, Peyrot V, Andreu J M. Stathmin and interfacial microtubule inhibitors recognize a naturally curved conformation of tubulin dimers. *J Biol Chem* 2010; 285: 31672-81.
5. Breuzard, G.; Hubert, P.; Nouar, R.; De Bessa, T.; Devred, F.; Barbier, P.; Sturgis, J. N. Peyrot, V. Molecular mechanisms of Tau binding to microtubules and its role in microtubule dynamics in live cells. *J Cell Sci* 2013; 126: 2810-9.

6. Jordan M A, Wilson L. Microtubules as a target for anticancer drugs. *Nat Rev Cancer* 2004; 4: 253–65.
7. Jordan M A, Kamath K. How do microtubule-targeted drugs work? An overview. *Curr Cancer Drug Targets* 2007; 7: 730-742.
8. van Vuuren R J, Visagie M H, Theron A E, Joubert A M. Antimitotic drugs in the treatment of cancer. *Cancer Chemother Pharmacol* 2015; 76: 1101–12.
9. Jordan M A. Mechanism of action of antitumor drugs that interact with microtubules and tubulin. *Curr Med Chem AntiCancer Agents* 2002; 2: 1-17.
10. Pettit G R, Singh S B, Boyd M R, Hamel E, Pettit R K, Schmidt J M, Hogan F. Antineoplastic Agents. 291. Isolation and synthesis of combretastatins A-4, A-5, and A-6 (1a). *J Med Chem* 1995; 38: 1666-72.
11. Lin C M, Singh S B, Chu P S, Dempcy R O, Schmidt J M, Pettit G R, Hamel E. Interactions of tubulin with potent natural and synthetic analogs of the antimitotic agent combretastatin: a structure-activity study. *Mol Pharmacol* 1988; 34: 200-8.
12. Tozer G M, Kanthou C, Parkins C S, Hill S A. The biology of the combretastatins as tumour vascular targeting agents. *Int J Exp Pathol* 2002; 83: 21–38.
13. Pettit G R, Singh S B, Niven M L, Hamel E, Schmidt J M. Isolation, structure, and synthesis of combretastatins A-1 and B-1, potent new inhibitors of microtubule assembly, derived from *Combretum caffrum*. *J Nat Prod* 1987; 50:119-31.
14. Hinnen P, Eskens F A L M. Vascular disrupting agents in clinical development. *Br J Cancer* 2007; 96: 1159–65.
15. Kanthou C, Tozer G M. Tumour targeting by microtubule-depolymerising vascular disrupting agents. *Expert Opin Ther Targets* 2007; 11: 1443-57.
16. Banerjee S, Wang Z, Mohammad M, Sarkar F H, Mohammad R M. Efficacy of selected natural products as therapeutic agents against cancer. *J Nat Prod* 2008; 71: 492-6.
17. Butler M S. Natural products to drugs: natural product-derived compounds in clinical trials. *Nat Prod Rep* 2008; 25: 475–516.
18. Sun M, Xu Q, Xu J, Wu Y, Wang Y, Zuo D, Guan Q, Bao K, Wang J, Wu Y, Zhang W. Synthesis and bioevaluation of N,4-diaryl-1,3-thiazole-2-amines as tubulin inhibitors with potent antiproliferative activity. *PLoS One* 2017; 12: e0174006.

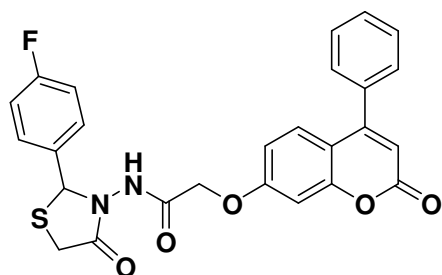
19. Banimustafa M, Kheirollahi A, Safavi M, Kabudanian Ardestani S, Aryapour H, Foroumadi A, Emami S. Synthesis and biological evaluation of 3-(trimethoxyphenyl)-2(3H)-thiazole thiones as combretastatin analogs. *Eur J Med Chem* 2013; 70: 692-702.
20. Romagnoli R, Baraldi PG, Brancale A, Ricci A, Hamel E, Bortolozzi R, Basso G, Viola G. Convergent synthesis and biological evaluation of 2-amino-4-(3',4',5'-trimethoxyphenyl)-5-aryl thiazoles as microtubule targeting agents. *J Med Chem* 2011; 54:5144-53.
21. Sharma S, Gupta M K, Saxena A K, Bedi P M. Thiazolidinone constraint combretastatin analogs as novel antitubulin agents: Design, synthesis, biological evaluation and docking studies. *Anticancer Agents Med Chem* 2017; 17: 230-40.
22. Batran R Z, Dawood D H, El-Seginy S A, Maher T J, Gugnani K S, Rondon-Ortiz A N. Coumarinyl pyranopyrimidines as new neuropeptide S receptor antagonists; design, synthesis, homology and molecular docking. *Bioorg Chem* 2017; 75:274-90.
23. Abdelhafez O M, Amin K M, Ali H I, Maher T J, Batran R Z. Dopamine release and molecular modeling study of some coumarin derivatives. *Neurochem Int* 2011; 59: 906-12.
24. Abdelhafez OM, Amin KM, Ali HI, Abdalla MM, Batran RZ. Synthesis of new 7-oxycoumarin derivatives as potent and selective monoamine oxidase A inhibitors. *J Med Chem* 2012; 55:10424-36.
25. Abdelhafez O M, Amin K M, Batran R Z, Maher T J, Nada S A, Sethumadhavan S. Synthesis, anticoagulant and PIVKA-II induced by new 4-hydroxycoumarin derivatives. *Bioorg Med Chem* 2010; 18:3371-8.
26. Thakur A, Singla R, Jaitak V. Coumarins as anticancer agents: a review on synthetic strategies, mechanism of action and SAR studies. *Eur J Med Chem* 2015; 101: 476-95.
27. Abdel Latif N A, Batran R Z, Khedr M A, Abdalla M M. 3-Substituted-4-hydroxycoumarin as a new scaffold with potent CDK inhibition and promising anticancer effect: Synthesis, molecular modeling and QSAR studies. *Bioorg Chem* 2016; 67: 116-29.
28. Batran RZ, Dawood DH, El-Seginy SA, Ali MM, Maher TJ, Gugnani KS, Rondon-Ortiz AN. New Coumarin Derivatives as Anti-Breast and Anti-Cervical Cancer Agents Targeting VEGFR-2 and p38 α MAPK. *Arch Pharm (Weinheim)* 2017; 350: e1700064.
29. Bailly C, Bal C, Barbier P, Combes S, Finet JP, Hildebrand MP, Peyrot V, Wattez N. Synthesis and biological evaluation of 4-arylcoumarin analogues of combretastatins. *J Med Chem* 2003; 46: 5437-44.

30. Combes S, Barbier P, Douillard S, McLeer-Florin A, Bourgarel-Rey V, Pierson J T, Fedorov A Y, Finet J P, Boutonnat J, Peyrot V. Synthesis and biological evaluation of 4-arylcoumarin analogues of combretastatins. Part 2. *J Med Chem* 2011; 54: 3153-62.
31. Mutai P, Breuzard G, Pagano A, Allegro D, Peyrot V, Chibale K. Synthesis and biological evaluation of 4 arylcoumarin analogues as tubulin-targeting antitumor agents. *Bioorg Med Chem* 2017; 25:1652-65.
32. Rappl C, Barbier P, Bourgarel-Rey V, Grégoire C, Gilli R, Carre M, Combes S, Finet JP, Peyrot V. Interaction of 4-arylcoumarin analogues of combretastatins with microtubule network of HBL100 cells and binding to tubulin. *Biochemistry* 2006; 45:9210-8.
33. Jiang J, Zheng C, Zhu K, Liu J, Sun N, Wang C, Jiang H, Zhu J, Luo C, Zhou Y. Quantum chemistry calculation-aided structural optimization of combretastatin A-4-like tubulin polymerization inhibitors: improved stability and biological activity. *J Med Chem* 2015; 58:2538-46.
34. Gaspari R, Prota A E, Bargsten K, Cavalli A, Steinmetz M O. Structural Basis of cis- and trans-Combretastatin Binding to Tubulin. *Chem* 2017; 2: 2102–13.
35. Kennedy M J, Donehower R C, Rowinsky E K. Treatment of metastatic breast cancer with combination paclitaxel/cyclophosphamide. *Semin Oncol* 1995;22: 23-7.
36. Davidson N G. Single-agent paclitaxel at first relapse following adjuvant chemotherapy for breast cancer. *Semin Oncol* 1995; 22:2-6.
37. Jordan M A, Thrower D, Wilson L. Mechanism of inhibition of cell proliferation by Vinca alkaloids. *Cancer Res* 1991; 51:2212-22.
38. Dhamodharan R, Jordan M A, Thrower D, Wilson L, Wadsworth P. Vinblastine suppresses dynamics of individual microtubules in living interphase cells. *Mol Biol Cell* 1995; 6:1215-29.
39. Derry W B, Wilson L, Jordan M A. Substoichiometric binding of taxol suppresses microtubule dynamics. *Biochemistry* 1995; 34:2203-11.
40. Yvon A M, Wadsworth P, Jordan M A. Taxol suppresses dynamics of individual microtubules in living human tumor cells. *Mol Biol Cell* 1999; 10: 947-59.
41. Diab S, Teo T, Kumarasiri M, Li P, Yu M, Lam F, Basnet SK, Sykes MJ, Albrecht H, Milne R, Wang S. Discovery of 5-(2-(phenylamino)pyrimidin-4-yl)thiazol-2(3H)-one derivatives as potent Mnk2 inhibitors: synthesis, SAR analysis and biological evaluation. *ChemMedChem* 2014; 9: 962-72.

42. Lu Y, Chen J, Xiao M, Li W, Miller D D. An overview of tubulin inhibitors that interact with the colchicine binding site. *Pharm Res* 2012; 29: 2943-71.
43. Chang C H, Yu F Y, Wu T S, Wang L T, Liu B H. Mycotoxin citrinin induced cell cycle G2/M arrest and numerical chromosomal aberration associated with disruption of microtubule formation in human cells. *Toxicol Sci* 2011; 119: 84-92.
44. Hou Z J, Luo X, Zhang W, Peng F, Cui B, Wu S J, Zheng F M, Xu J, Xu L Z, Long Z J, Wang X T, Li G H, Wan X Y, Yang Y L, Liu Q. Flubendazole, FDA-approved anthelmintic, targets breast cancer stem-like cells. *Oncotarget* 2015; 6: 6326-40.
45. Magalhães H I, Wilke D V, Bezerra D P, Cavalcanti B C, Rotta R, de Lima D P, Beatriz A, Moraes M O, Diniz-Filho J, Pessoa C. (4-Methoxyphenyl)(3,4,5-trimethoxyphenyl)methanone inhibits tubulin polymerization, induces G2/M arrest, and triggers apoptosis in human leukemia HL-60 cells. *Toxicol Appl Pharmacol* 2013; 272:117-26.
46. Kumar S. Caspase function in programmed cell death. *Cell Death Differ* 2007; 14: 32-43.
47. Li J, Yuan J. Caspases in apoptosis and beyond. *Oncogene* 2008; 27:6194-206.
48. Lee D, Long S A, Adams J L, Chan G, Vaidya K S, Francis T A, Kikly K, Winkler J D, Sung C M, Debouck C, Richardson S, Levy M A, DeWolf W E Jr, Keller P M, Tomaszek T, Head M S, Ryan M D, Haltiwanger R C, Liang P H, Janson C A, McDevitt P J, Johanson K, Concha N O, Chan W, Abdel-Meguid S S, Badger A M, Lark M W, Nadeau D P, Suva L J, Gowen M, Nuttall M E. Potent and selective nonpeptide inhibitors of caspases 3 and 7 inhibit apoptosis and maintain cell functionality. *J Biol Chem* 2000; 275:16007-14.
49. Nguyen T L, McGrath C A, Hermone R, Burnett J C, Zaharevitz D W, Day B W, Wipf, P, Hamel E, Gussio R. A common pharmacophore for a diverse set of colchicine site inhibitors using a structure-based approach. *J Med Chem* 2005; 48: 6107-16.
50. Zhang X, Kong Y, Zhang J, Su M, Zhou Y, Zang Y, Li J, Chen Y, Fang Y, Zhang X, Lu W, Design, synthesis and biological evaluation of colchicines derivatives as novel tubulin and histone deacetylase dual inhibitors. *Eur Med Chem* 2015; 95: 127-35.
51. Lipinski C A, Lombardo F, Dominy B W, Feeney P J. Experimental and computational approaches to estimate solubility and permeability in drug discovery and development settings. *Adv Drug Deliv Rev* 1997; 23: 3-25.
52. Palm K, Stenberg P, Luthman K, Artursson P. Polar molecular surface properties predict the intestinal absorption of drugs in humans. *Pharm Res* 1997; 14: 568-71.

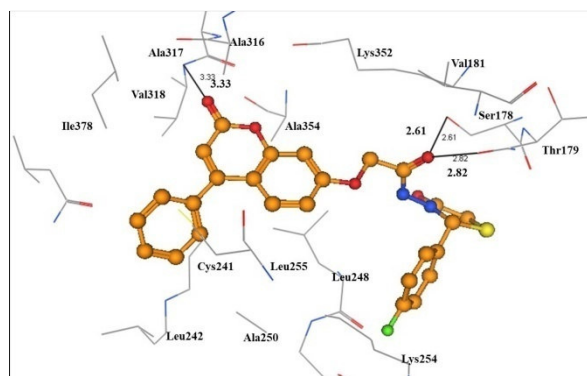
53. Walters W P, Stahl M T, Murcko M A. Virtual screening-an overview. *Drug Discov Today* 1998; 3: 160-78.
54. Hassan G S, Farag N A, Hegazy G H, Arafa R K. Design and synthesis of novel benzopyran-2-one derivatives of expected antimicrobial activity through DNA gyrase-B inhibition. *Arch Pharm (Weinheim)* 2008; 341:725-33.
55. Mosmann T. Rapid colorimetric assay for cellular growth and survival: application to proliferation and cytotoxicity assays. *J Immunol Methods* 1983;65:55-63.
56. Thabrew M I, Hughes R D, McFarlane I G. Screening of hepatoprotective plant components using a HepG2 cell cytotoxicity assay. *J Pharm Pharmacol* 1997; 49:1132-5.
57. Moustafa SM, Menshawi BM, Wassel GM, Mahmoud K, Mounier MM. Screening of some plants in Egypt for their cytotoxicity against four human cancer cell lines. *Int J Pharm Tech Res* 2014; 6: 1074-84.
58. Liliom K, Lehotzky A, Molnár A, Ovádi J. Characterization of tubulin-alkaloid interactions by enzyme-linked immunosorbent assay. *Anal Biochem* 1995; 228:18-26.

Graphical Abstract



3a

IC_{50} -MCF-7= 11.1 μ g/mL
 IC_{50} -TUBb= 9.37 μ M
Apoptosis induction
Cell cycle arrest at G2/M phase
Upregulation of caspase-7



Highlights

- A new set of 4-phenylcoumarins was designed and synthesized.
- Cytotoxic effects against MCF-7 were assessed.
- Compounds **3a**, **3b** and **3f** were potent TUBb polymerization inhibitors.
- **3a** induced cell cycle arrest at G2/M phase and activated caspase-7.
- Molecular docking and dynamics studies were performed.

ACCEPTED MANUSCRIPT